


 Cite this: *RSC Adv.*, 2021, **11**, 29247

# Metal–organic framework based electrode materials for lithium-ion batteries: a review

 Rimsha Mehek,<sup>a</sup> Naseem Iqbal,<sup>b</sup> Tayyaba Noor,<sup>b</sup> M. Zain Bin Amjad,<sup>a</sup> Ghulam Ali,<sup>a</sup> K. Vignarooban<sup>c</sup> and M. Abdullah Khan<sup>d</sup>

Metal–organic frameworks (MOFs) with efficient surface and structural properties have risen as a distinctive class of porous materials through the last few decades, which has enabled MOFs to gain attention in a wide range of applications like drug delivery, gas separation and storage, catalysis and sensors. Likewise, they have also emerged as efficient active materials in energy storage devices owing to their remarkable conducting properties. Metal–organic frameworks (MOFs) have garnered great interest in high-energy-density rechargeable batteries and super-capacitors. Herein the study presents their expanding diversity, structures and chemical compositions which can be tuned at the molecular level. It also aims to evaluate their inherently porous framework and how it facilitates electronic and ionic transportation through the charging and discharging cycles of lithium-ion batteries. In this review we have summarized the various synthesis paths to achieve a particular metal–organic framework. This study focuses mainly on the implementation of metal–organic frameworks as efficient anode and cathode materials for lithium-ion batteries (LIBs) with an evaluation of their influence on cyclic stability and discharge capacity. For this purpose, a brief assessment is made of recent developments in metal–organic frameworks as anode or cathode materials for lithium-ion batteries which would provide enlightenment in optimizing the reaction conditions for designing a MOF structure for the battery community and electrochemical energy storage applications.

 Received 30th June 2021  
 Accepted 20th August 2021

DOI: 10.1039/d1ra05073g

[rsc.li/rsc-advances](http://rsc.li/rsc-advances)

## 1. Introduction

### 1.1. Energy scenario – challenges and prospects

Energy consumption by human society largely depends upon conventional energy resources which are depleting at a faster pace. These resources are not enough to fulfil our energy needs. Therefore, an increasingly growing portion of the current energy consumption is taken up by renewable energy resources such as solar, hydro and wind power. The power output of these energy resources is highly fluctuating and intermittent which invites the parallel implementation of electrochemical energy conversion and storage technologies, such as fuel cells, rechargeable batteries and electrochemical capacitors. These storage technologies are making sustainable energy utilization easy and efficient.<sup>1,2</sup> The electricity generated from any renewable source like solar or wind power can be efficiently stored in rechargeable batteries and electrochemical capacitors in the form of

chemical energy and later can later be released from the system or converted to electricity by electrolyzers or regenerated by fuel cells.<sup>1</sup> The electrochemical devices include the following three functional parts. Electrodes (cathode and anode) are the main part where the major electrochemical processes take place such as energy storage in the case of batteries/capacitors and electrocatalysts that support reactions in fuel cells, and an electrolyte that allows the transport of ions and blocks electronic conduction to complete the electric circuit.<sup>3</sup> In principle, physical properties, such as ionic or electronic conductivity, and electrical properties, such as the catalytic and redox activity of the functional materials implanted into these components, determine the device's performance.<sup>4–6</sup> Hence, the search for a material with suitable features has been a primary quest in developing efficient technologies related to energy systems.

### 1.2. Evolution of lithium-ion batteries (LIBs)

The progress of implantable medical devices, high-energy and high-power sources required for military purposes and the exponential growth of the portable electronics market are some of the major reasons behind the research and innovation for the growth of batteries. Fig. 1 summarizes the evolution of lithium-ion batteries over the period of sixty years. It outlines all the major strategies devised to achieve better performance and higher capacity. In the early 1960s, medical devices including

<sup>a</sup>U.S.-Pakistan Center for Advanced Studies in Energy (USPCAS-E), National University of Sciences and Technology (NUST), H-12 Campus, Islamabad 44000, Pakistan. E-mail: naseem@uscpe.nust.edu.pk; Tel: +92 51 9085 5281

<sup>b</sup>School of Chemical and Materials Engineering (SCME), National University of Sciences and Technology (NUST), Islamabad, Pakistan

<sup>c</sup>Department of Physics, Faculty of Science, University of Jaffna, Jaffna 40000, Sri Lanka

<sup>d</sup>Renewable Energy Advancement Laboratory (REAL), Department of Environmental Sciences, Quaid-i-Azam University, Islamabad 45320, Pakistan





Fig. 1 Historical evolution and advances in lithium-ion batteries. Reproduced from ref. 2 with permission from Royal Society of Chemistry, Copyright 2013.

pace-makers relied on the use of the zinc–mercury batteries available at that time.<sup>7</sup> Then a breakthrough was achieved with the discovery of lithium as a strong candidate for an electrode material with the highest theoretical capacity, which was  $3860 \text{ A h kg}^{-1}$  as compared with that of zinc which was  $820 \text{ A h kg}^{-1}$ .<sup>8</sup> On a practical level, achieving this much capacity in lithium batteries faces many hurdles. The first problem associated with lithium is that it is not compatible with moisture.<sup>9</sup> Therefore, a battery set-up using lithium as one electrode needs more stable non-aqueous electrolyte systems. With the discovery of lithium, innovation started with lithium in combination with other reactive and active alternatives.<sup>10</sup> For example, lithium iodine batteries had lithium as the anode and iodine as the cathode with an energy density of  $250 \text{ W h kg}^{-1}$ , which was five times greater than that of zinc–mercury batteries.<sup>11–13</sup> Thus, an era of lithium anode based batteries with high capacity started with a promising future. Researchers have also tested lithium batteries with uncommon cathode materials like soluble reagents, e.g., sulfur dioxide ( $\text{SO}_2$ ), and liquid reagents, such as thionyl chloride ( $\text{SOCl}_2$ ) or sulfuryl chloride ( $\text{SO}_2\text{Cl}_2$ ).<sup>14</sup> The reason behind the deployment of lithium in the 1970s was that it was easily usable in electronic devices such as electronic watches, cameras, toys and portable devices.<sup>13</sup> All these applications were satisfied by an LIB with manganese dioxide as the cathode material fabricated

as a coin cell type of battery. All these battery technologies are considered as primary batteries whose success led to secondary batteries.<sup>15</sup> Later in 1978, a breakthrough was achieved with the development of intercalation electrode types which led to a great number of secondary or rechargeable LIBs. The intercalation process is based on the reversible inclusion concept in which during the first half-cycle lithium ions are taken in within the open structure of the host matrix and then given out during the second half-cycle of the battery.<sup>16,17</sup> After some time, in the late 1970s, keeping up with the phenomenon of intercalation, the first commercial rechargeable lithium battery with a  $\text{TiS}_2$  cathode was made by the Exxon company in the USA.<sup>18</sup> Similarly, another company named Moli Energy in Canada also made lithium batteries with  $\text{MoS}_2$  as the cathode material.<sup>19</sup> There were some irregularities observed in these batteries, like overheating and ultimately explosions in lithium batteries with an SEI (solid electrolyte interphase).<sup>20</sup> To overcome this issue, efforts started in 1978, ultimately introducing the concept of polymer electrolytes.<sup>21,22</sup> A polymeric electrolyte is a complex compound of a lithium salt and a coordinating polymer host. In the late 1970s, the concept of rocking-chair batteries also emerged as a part of intercalation-based lithium batteries which were practically demonstrated in the 1980s.<sup>23,24</sup>



Table 1 General properties of an efficient cathode and anode material for lithium-ion batteries

| Sr. # | Cathode  | Anode  |
|-------|--|--|
| 1     | Better reversible and irreversible capacity              | High thermal stability   |
| 2     | High rate capability and more cycle life                 | Excellent compatibility with electrolyte                       |
| 3     | Safe, less costly and non-toxic                          | Fast diffusion rate for lithium ions                           |
| 4     | Zero strain (almost no volume change)                    | Maximum reversibility of Li ions during cycling                |
| 5     | Stable structure   | Highest possible potential energy of anode material            |
| 6     | Uniform phase distribution during charge–discharge cycle | Easy to synthesize and cost effective                          |
| 7     | Maximum lithium flow                                     | High electrical, electronic, and ionic conductivity            |
| 8     | Improving electronic percolation and ionic conductivity  | Fermi level of the anode material should be as low as possible |

More than 10 years later, in 1991, the Japanese company Sony manufactured a lithium battery which had graphite as the anode and lithium cobalt oxide as the cathode.<sup>25,26</sup> With different variations in the cathode and lithium-based anode materials, presenting better performance, capacity or density, the timeline went on. In the twenty-first century, the variations were mainly in having anode materials which were derivatives of lithium with transition and/or non-transition metals and their oxides.<sup>27</sup> There were major variations on the cathode side as well. Graphite alternatives were introduced with better intercalation of lithium-sinking capabilities. The concept of hard and soft carbon-based cathodes did not come in until the end of 2010 (ref. 28) but due to the drop in capacity with pure carbon structures over time, the concept of alloy materials like Si alloys was introduced to overcome this problem. Until now, research and innovation have been more focused on using alloy materials as the cathode to provide better performance and promising long-term capacity.<sup>29</sup>

The interdependence of potential difference, electrochemical reaction and the ion–electrode interaction narrows down to a study of the type and necessary properties of materials used as electrodes for LIBs. For high-capacity anodes and cathodes, the properties mentioned in Table 1 are necessary to provide better ion–electrode interaction leading to better charge storage.<sup>30</sup>

LIBs have been seen in much of an era of metallic anodes and for logically good reasons.<sup>31</sup> To attain the maximum specific and volumetric capacities, it is necessary to pack the atoms in as small a space as possible. The most efficient way to do that is to use a pure solid metallic material which ultimately gives the maximum theoretical capacity available. The use of metallic anode materials is also subject to some issues. Different metals encounter different problems, but all of them mostly root from the common issue that is the highly reactive surface of metals. Apart from graphite, the most studied metallic anode materials are lithium, sodium, magnesium, aluminum, and alloying materials.

### 1.3. Introduction to metal organic framework

Metal–organic frameworks (MOFs) are a class of porous materials first introduced by O. M. Yaghi and his co-workers in 1995.<sup>32</sup> They have gained immense attention during the past two decades. These materials are crystalline structures assembled in the form of a network containing a central metal unit known as a secondary building unit and organic linkers. By varying the metal unit and organic linker, one can generate

a huge number of such compounds. More than 20 000 different MOFs have been created and this number is still growing.<sup>33</sup> MOFs are prominent as an expanding group of synthetic crystals with ultrahigh porosity (up to 90% free volume) and large internal surface areas, expanding to over 6000 m<sup>2</sup> g<sup>−1</sup>. These properties, coupled with the extraordinary degree of diversity in both organic and inorganic components of their structures, make MOFs of interest for exploitation in many potential applications in clean energy technologies.<sup>34,35</sup> Metal–organic frameworks and their derivatives are porous materials which have gained a lot of attention for a very long time because of their simple synthesis route, controllable structure, very high porosity, low energy consumption and high surface area.<sup>36–38</sup> These structures have caused great hype because of their controllable structures, tunable properties, and diverse applications. Basically, when a researcher has the margin to modify the structure of the compound, they can also command the product to work for a certain application. Due to such diversity present in MOF materials, they have found applications in gas storage, catalysis, sensing, magnetism, drug delivery, electrocatalysis and carbon dioxide reduction<sup>39–50</sup> (Fig. 2).



Fig. 2 Applications of MOFs and their composites in various energy applications. Reproduced from ref. 34 with permission from Elsevier, Copyright 2017.



MOFs can be synthesized as nanoparticles and can also form nanocomposites with additional active nano-components. Apart from that MOFs can also be used as sacrificial materials to derive different nanoporous structures by thermal treatment.<sup>51–53</sup> Such diversity of structure and composition leads to the diverse and tunable functionality of MOFs. MOFs that contain redox-activated metal centers, typically first-line transition metals (Fe, Co, Ni, Mn *etc.*), are of particular interest for delivering electrochemical activity. Therefore, MOFs are found to be considerably good candidates for electrode materials in LIBs<sup>55,54</sup> and all these structural strategies involving MOFs are promising for better lithium storage in the case of LIBs. Ion-selective MOF membranes have been used as electrodes, electrolytes, and catalytic material for almost all types of lithium-based batteries (Fig. 3).

MOFs suffer from relatively inadequate electronic conductivity and chemical instability; therefore, they have also been extensively converted into metal compounds and carbonaceous materials or their composites.<sup>56–60</sup> These MOF-derived functional materials usually exhibit remarkable advantages originating from their microstructures or nanostructures, showing great potential for energy-related technological applications. Although MOF-derived carbonaceous electrode materials are of great interest, they also come with their own baggage of problems and limitations. A MOF carbonized at a lower temperature results in a poorly graphitized composite structure. This leads to high resistance and poor electrochemical performance. On the other hand, carbonization at high temperature results in highly conductive carbonaceous material but it also converts the metal oxide component into metal nanoparticles which have poor capacitance.<sup>61</sup> To overcome these issues, optimization of carbonization temperature and temperature ramp rate is required according to the type of MOF structure and metallic unit being treated.

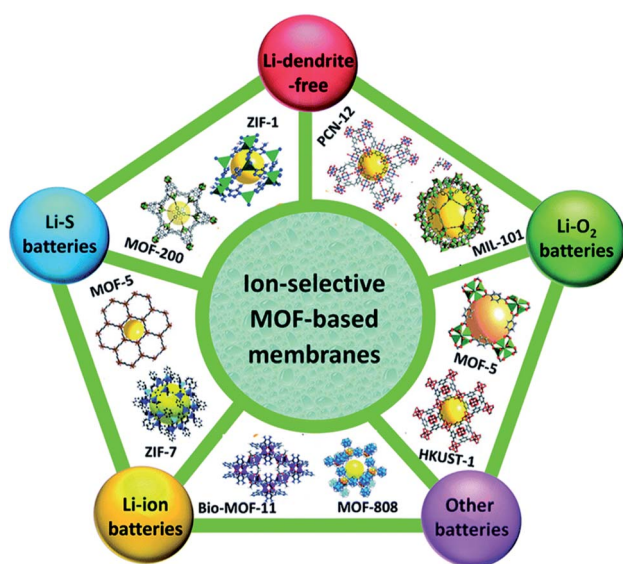


Fig. 3 MOF-incorporating electrode applications in batteries. Reproduced from ref. 55 with permission from Royal Society of Chemistry, Copyright 2019.

**1.3.1. Synthesis routes of MOFs.** The synthesis of a MOF material is a matter of controlling the reaction conditions to a certain level where the structures can be developed according to the researchers' desires or the application concerned. Various MOFs can be produced by carefully choosing the organic or inorganic linker around the selected metal of interest. The structure and pore size are tuned by controlling the synthesis conditions, post-synthetic modifications, favorable chemical activity *etc.* The choice of synthesis route depends entirely upon the desired property in the MOF structure. Thus, a different strategy is adopted to achieve a unique property in a MOF structure.

The energy required to produce the MOF can be of any type: electric potential, electromagnetic radiation, or mechanical waves, but thermal energy is considered the most appropriate for the production of a MOF. The energy source is closely related to the other reaction conditions like duration, pressure, and energy per molecule that are being introduced into the system. Fig. 4 shows the effect of treatment and reaction time on the development of different structures. Each of these parameters has an individual influence on the properties of the product and thus all the parameters need to be well studied in advance.<sup>62</sup>

As far as the choice of precursors is concerned, MOFs being organic and inorganic hybrid materials are generated by combining an inorganic part, *i.e.*, a metal (such as  $\text{Fe}^{2+}$ ,  $\text{Co}^{2+}$ ,  $\text{Ni}^{2+}$ ,  $\text{Cu}^{2+}$ ,  $\text{Zn}^{2+}$ ,  $\text{Mg}^{2+}$ ,  $\text{Mn}^{2+}$ ,  $\text{Al}^{3+}$ , or  $\text{Fe}^{3+}$ ) and an organic part (usually a mono-, di-, tri- or tetravalent ligand containing a heteroatom like oxygen or nitrogen).

Apart from synthesizing pristine metal-organic frameworks, MOF-derived nanoarchitectures with a unique porous surface or hollow structures also involve some important thermal treatment strategies. For example, a MOF-supported annealing reaction resulting in core-shell hollow  $\text{Fe}_2\text{O}_3/\text{Co}_3\text{O}_4$  microcubes has found potential applications in lithium batteries.<sup>64,65</sup> Similarly, annealing the core-shell Fe-Co-Ni trimetallic MOF resulted in  $\text{Fe}_2\text{O}_3@\text{NiCo}_2\text{O}_4$  which represented an excellent capacity of 1079.6 mA h  $\text{g}^{-1}$ .<sup>66</sup> A ZnO/ZnFe<sub>2</sub>O<sub>4</sub>/C based core-shell spinel oxide derived from porous carbon through facile green synthesis also exhibited improved cyclic performance with a reversible capacities of 837 and 988 mA h  $\text{g}^{-1}$  after 100

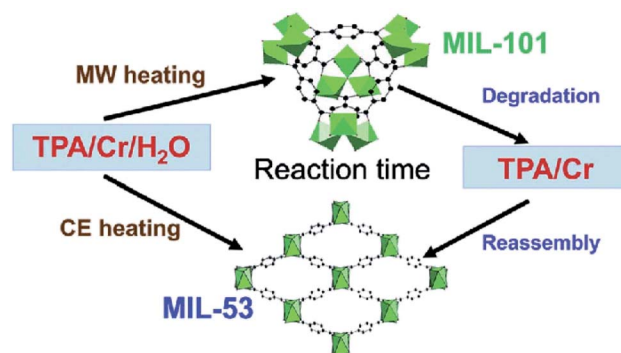


Fig. 4 Various morphologies of MOFs obtained by tuning reaction conditions. Reproduced from ref. 63 with permission from Royal Society of Chemistry, Copyright 2018.



discharge cycles.<sup>67,68</sup> A unique ZnO/ZnCo<sub>2</sub>O<sub>4</sub> core-shell nanostructured architecture derived from a core-shell MOF also exhibited 669 mA h g<sup>-1</sup> after 250 cycles.<sup>69</sup> A detailed overview of some important schemes of preparation with their resulting morphologies is discussed in the next section.

**1.3.2. Morphology, crystal structure and chemistries involved in MOFs.** Whenever there is a new breakthrough or an extension to the previous work on MOFs, there is an extreme elaboration about how enriched the structure is with topological considerations depicting the structure, not only in terms of classical chemistry like atoms, bonds, and crystal structure, but also in terms of the periodic networks involved. This is only one of several ways to describe a structure. There are plenty more

ways to describe the morphology of the framework with certain advantages and disadvantages.<sup>70</sup>

There are certain experimental purposes involved in devising a particular structure for a metal-organic framework. These experimental objectives are driven mostly by a certain motivation, which has always been present in elaborating the structural or functional feature of a material with the aid of structural chemistry and surface chemistry.<sup>71</sup> One structural representation can be based upon sphere or rod packing, another on a corner-, edge- or face-centered coordination polymer (Fig. 5). It is also notable that this concept of structural representation on the basis of structural packing is becoming less applicable because of the increasing level of irregularity,

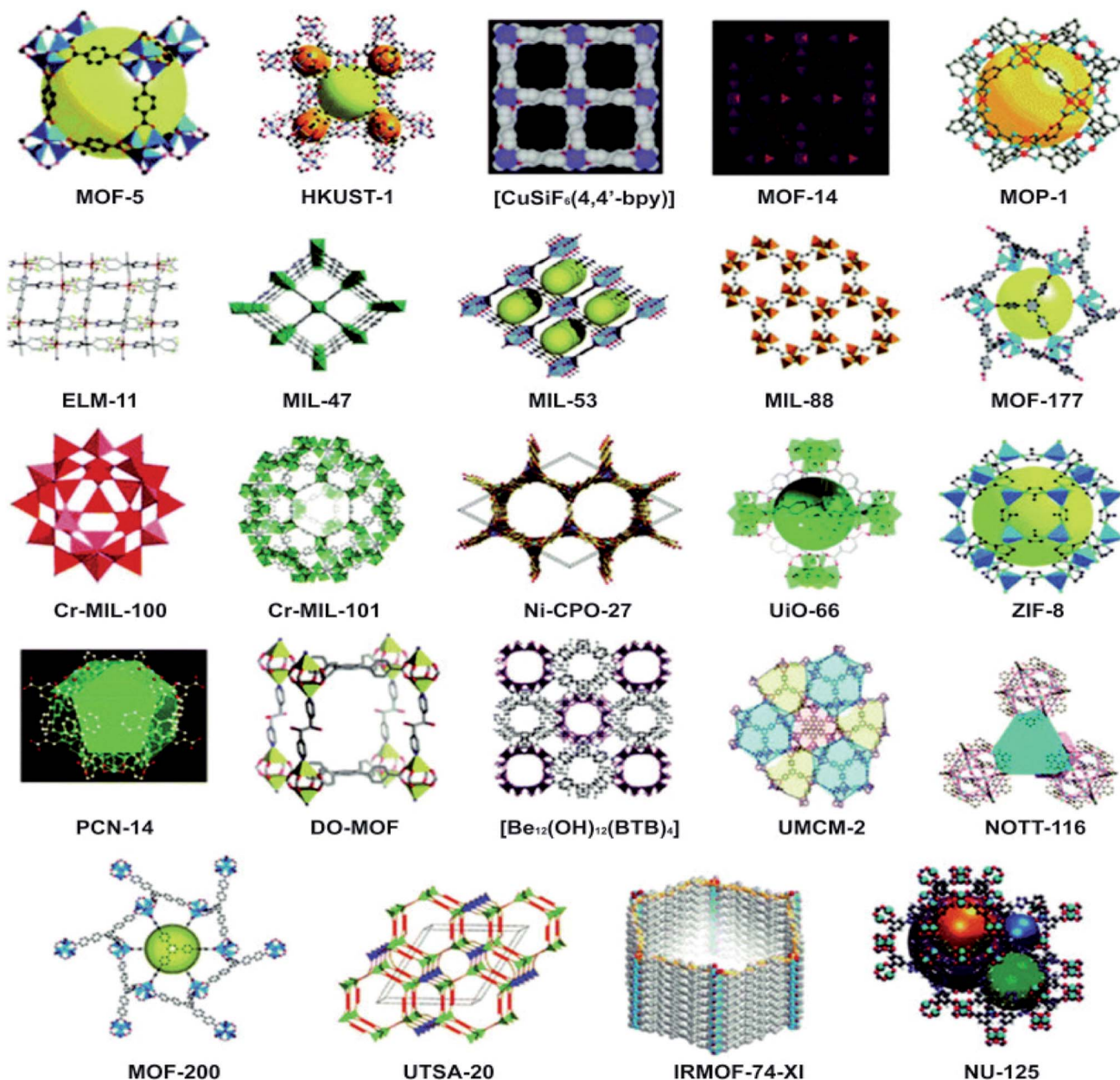


Fig. 5 Various structures attained in metal-organic frameworks. Reproduced from ref. 73 with permission from Royal Society of Chemistry, Copyright 2015.





**Fig. 6** Various morphologies of MOFs under SEM of (a) cobalt metal-organic framework, reproduced from ref. 76 with permission from Elsevier, Copyright 2017; (b) MOF-5 crystals, reproduced from ref. 79 with permission from Nature, Copyright 2011; (c) a MOF with a cauliflower morphology, reproduced from ref. 80 with permission from Elsevier, Copyright 2016 and (d) stable porous hollow nanocubes of Au@Zn/Ni-MOF-2 core-shell, reproduced from ref. 81 with permission from American Chemical Society, Copyright 2021.

degree of porosity and greater involvement of covalent or hydrogen bonds in the compound.<sup>72</sup>

The metal-organic framework consists of both organic and inorganic building units. The inorganic entity is the central metal atom, also known as the secondary building unit (SBU). The organic linkers are the ones that make the main framework around the metallic center. They may be carboxylates, sulfonates, phosphates *etc.* These act as coordinating ligands. The framework topology attained in the end is governed by both the organic and the inorganic subunits. The presence of voids/spaces within the structures plays an important role in the chemical behavior of the material. MOFs with larger spaces result in interpenetrating structures. The pore size is also very important in this regard. The selection of the metal entity, the

reaction conditions and much more are responsible for tailoring the final outlook of the porous structure.

A large number of SBU geometries are available, where each provides a different number of connection points to the ligands. As a result, different crystal structures are achieved. These include trigonal prisms and octahedral shapes (six points), paddle-wheel-type square shapes (four points), and triangular shapes (three points). In bridged structures, a ligand is also capable of connecting with the metal through more than one vacant position (bidentate, tridentate, tetradentate, or polydentate). All of these variations end up giving rise to interesting porous morphologies likely to have many important applications in a variety of fields. Careful observation under a scanning electron microscope (SEM) represents the interesting morphologies of MOFs (Fig. 6).<sup>74–77</sup> MOFs tend to exhibit properties both physical and chemical which depend upon the size of the particles that cannot be observed in the bulk form. Whether used in the form of support, substrate, or sacrificial compounds, they immobilize the active functional material and produce highly controllable nanostructures to gain new momentum specifically for energy applications.<sup>78</sup>

To achieve the unique and effective architecture of hollow, porous or core-shell MOF-based structures for better electrochemical performance and improved conductivity for lithium-ion batteries, many strategies have been tested: for instance, the ship-in-a-bottle strategy. Qin *et al.* adopted a one-step strategy to achieve hollow Au@Zn/Ni-MOF-2 core-shell nanocubes.<sup>81</sup> The hollow cavity enables mass transfer while the outer shell achieves molecular-size selectivity. The hollow structure of the nanocubes with a particle size of around 500 nm is clear from the SEM images in Fig. 7(b) and (c). The nanocube-type structure is likely to offer better structural and thermal stability and better cyclability.

To achieve enhanced lithium storage and transport for lithium-ion batteries, Zhang *et al.* designed a multi-step synthesis process to prepare a core-shell PCNF@SnO<sub>2</sub>@CN nanofiber with a hierarchical porous coaxial structure (Fig. 8) which showed excellent rate capability with a capacity of 962 mA h g<sup>-1</sup>.<sup>82</sup> The introduction of graphitized carbon improves the conductivity and enables fast charge transport.

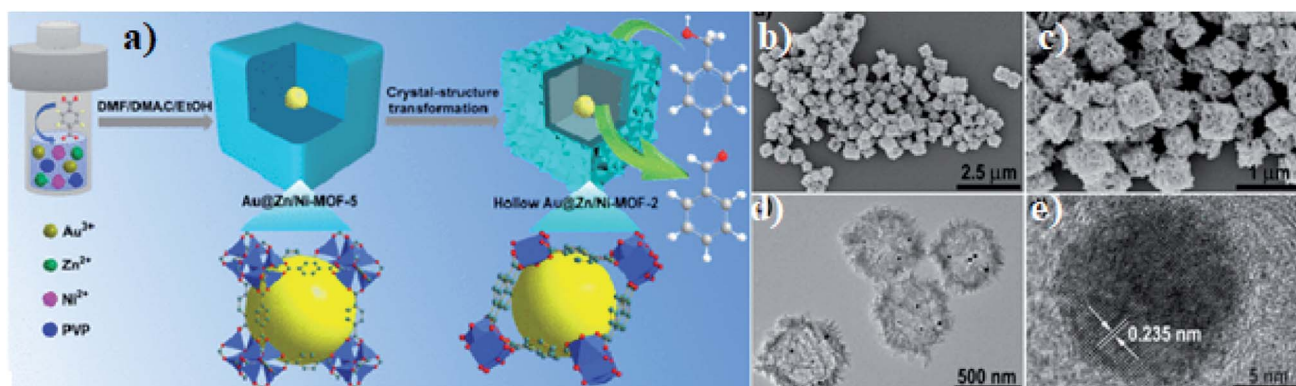


**Fig. 7** (a) Scheme of preparation of a hollow Au@Zn/Ni-MOF-2 core-shell nanoreactor, (b and c) SEM and (d and e) TEM of hollow Au@Zn/Ni-MOF-2 core-shell nanocubes. Reproduced from ref. 81 with permission from American Chemical Society, Copyright 2021.





Fig. 8 (a) Schematic illustration of the preparation of PCNF@SnO<sub>2</sub>@CN nanofibers, (b) SEM and (c) TEM of PCNF nanofibers, (d) SEM of PCNF@SnO<sub>2</sub>@CN nanofibers. Reproduced from ref. 83 with permission from Elsevier, Copyright 2021.

The hard carbon shell prevents the expansion of SnO<sub>2</sub> enabling better cycling performance. Such a one-dimensional porous structure also helps to avoid particle agglomeration during the charge/discharge process, keeping the structural integrity up to the mark.

Zeng *et al.* adopted a simple self-assembly technique to develop heteropolyanions within the ZIF-8 cavity labelled as ZnSe/MoSe<sub>2</sub>@C, which exhibited remarkable capacity in metal-ion batteries.<sup>83</sup> A hierarchical hollow porous nanostructure with a relatively homogeneous distribution was observed under SEM (Fig. 9). The active material exhibited a large capacity of 524 mA h g<sup>-1</sup> after 600 cycles in lithium-ion batteries and 468 mA h g<sup>-1</sup> after 50 cycles in sodium-ion batteries. The novel nano-architecture of the derived material aids in overcoming the sluggish reaction kinetics and relieves the volume strain during the charge/discharge cycles for LIBs. The few-layered MoSe<sub>2</sub> and carbon matrix obtained by *in situ* carbonization provides a unique buffering mechanism and partial pseudo-capacitance contribution.

Si nanoparticles and a carbon shell were successively deposited on CoMOF-D *via* the CVD method and denoted as CoMOF-

D@Si@C by Yan *et al.*<sup>84</sup> The inner porous graphitized structure and outer homogeneous carbon shell are responsible for enhanced electrical conductivity and extended volume expansion of Si. Such a delicate core-shell structure is believed to show a superior reversible capacity of 1493 mA h g<sup>-1</sup> after 400 cycles and excellent rate capability as an anode material for LIBs. The outer carbon shell, inner porous pyrolytic MOF structure and uniform Si deposition result in a unique stable architecture (Fig. 10) which maintains its structural stability and provides constructive conductivity during cycling processes.

## 2. Review of MOF-based electrode materials for LIBs

### 2.1. MOFs as electrode material for Li-ion batteries

In the last decade, electrochemical energy conversion and storage devices have gained a lot of attention. Among all such devices and energy solutions, the most studied are LIBs. The evolution of LIBs has already been discussed in previous sections. Here, the evolution of MOFs and the alternative chemistries related to or derived from them as potential electrode materials are the main focus.<sup>85</sup>

Rechargeable batteries and electrochemical capacitors are two primary types of electrochemical energy storage devices. Lithium-ion batteries (LIBs), being one of the modern battery types, are the center of research and development in the field of energy storage. The charging and discharging mechanism in LIBs relies on the reversible shuttling of lithium ions between two electrodes, offering high energy and power densities.<sup>86</sup> Lithium ions are de-intercalated from the cathode when LIBs are charging. Then, the de-intercalated lithium ions move through the electrolyte and intercalate at the anode. During this



Fig. 9 (a) SEM and (b) TEM of ZnSe/MoSe<sub>2</sub>@C showing a well-defined polyhedral structure. Reproduced from ref. 83 with permission from Royal Society of Chemistry, Copyright 2019.



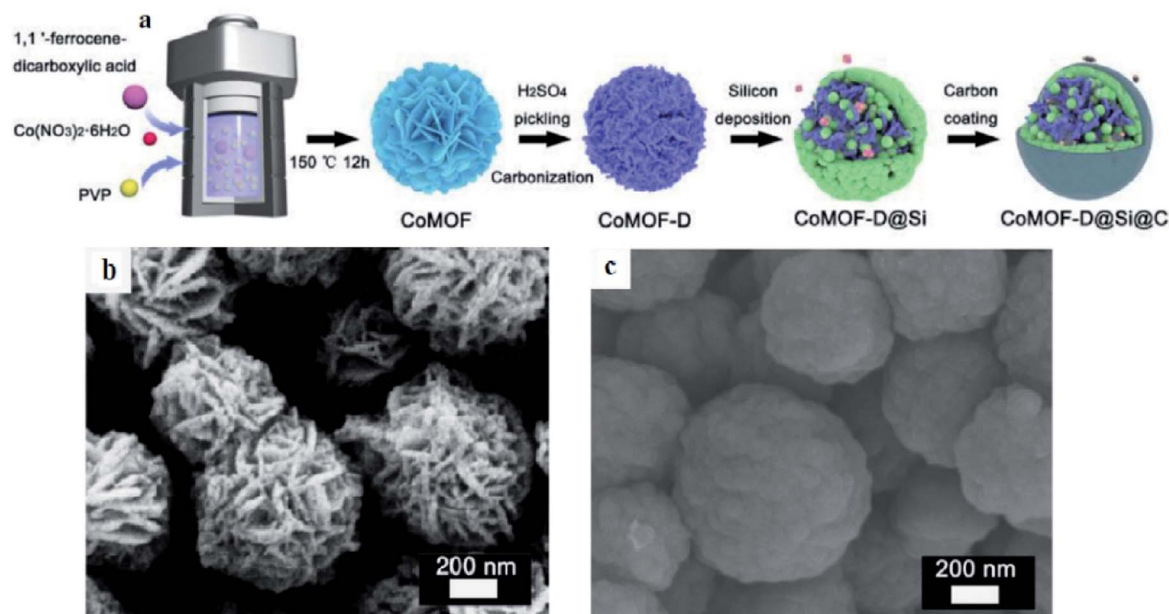


Fig. 10 (a) Schematic illustration of the synthesis of a CoMOF-D@Si@C composite; SEM images of (b) CoMOF and (c) CoMOF-D@Si@C composites. Reproduced from ref. 84 with permission from Elsevier, Copyright 2021.

process, LIBs obtain and store energy. When LIBs are discharging, the lithium ions move back to the cathode; LIBs release the stored energy during this process. The efficiency of these processes defines the overall efficiency of the battery. These processes are reinforced by the desired properties of the anode and cathode materials. Several studies have focused on finding the best electrode material in this regard. Conventional electrode materials suffer from a complicated synthesis process, limited energy/power densities and short cycle life. Therefore, materials like MOFs are promising electrode materials for LIBs because of their unique structure, high specific surface area, well-developed porosity and high lithium storage capacity.<sup>87,88</sup>

The tendency towards MOF materials in electrochemical applications has been reported by many researchers worldwide over the past few years.<sup>89</sup> One of the most important factors behind their better electrochemical properties is their larger surface area. The surface area of MOF structures ranges from 1000 to 10 000 m<sup>2</sup> g<sup>-1</sup> (ref. 90) which is higher than that of many conventional porous materials which are considered ideal for electrochemical applications. Another important factor is pore size. The average pore size is 9.8 nm, but this value is very flexible as the pore size can be varied by changing the length of the organic ligand around the metallic center.<sup>91</sup>

Another advantage associated with MOFs is their ability to provide redox-active sites by carefully choosing the metal center and organic linker. In fact, the versatility of MOFs in electrochemical applications comes from the fact that researchers have synthesized MOFs through different synthesis routes choosing from among a wide range of active metals and unique organic linkers; ultimately generating MOF structures with varied surface properties. By altering both the coordinating components, one can play with the chemistry of a MOF and use it to favor the electrochemical processes of a battery.<sup>74</sup> The morphology of a MOF can

also have an impact on the surface area, the number of active sites available and the kinetics involved during the ion–electrolyte interactions. Materials with such desirable properties as high surface area, active porosity, favorable surface chemistry and redox-active functional groups would always be a good choice for LIB electrodes. The high surface area of MOF materials provides maximum exposure to the electrolyte and a suitable pore size is beneficial for high flow rates of the electrolyte. The high porosity and crystallinity of MOFs provide larger spaces for accommodating lithium ions with better structural stability, leading to promising lithium storage.

Metal–organic frameworks have an extraordinary ability to host a range of ionic and elemental entities. This property along with their structural stability make them a good fit for storing lithium ions during the cycling of a lithium-ion battery. Also, the tunable porosity in these structures makes the diffusion of lithium ions more rapid and smoother – a property highly desirable for electrode materials in batteries. The functionality of MOFs is controllable due to the wide choice of organic sub-units and metallic centers.<sup>74</sup> This attribute has enabled scientists to prepare a wide range of MOFs good for electrochemical applications, especially as an electrode material for lithium-ion batteries. Initially pristine MOFs were tested for their lithium storage and transportation ability but a great deal of efficiency loss and low cyclic life was observed due to the lack of proper guest removal leading to pore clogging and ultimate framework decomposition.<sup>92</sup> To overcome this aspect, scientists started modifying MOF compounds by adding dopants or developing composites, such as metallic nanoparticles, metal oxides, carbon nanotubes, and graphene. All these compounds provided more stable and reversible active sites in addition to the enhanced porosity of the MOFs.<sup>93</sup> Another advance in this regard is using MOFs as precursors for the synthesis of sophisticated carbon-structures. As carbon-based





Table 2 List of pristine MOF structures and their performance as anode/cathode for lithium-ion batteries

| Sr. no. | Sample  | Electrode | Current density (mA g <sup>-1</sup> ) | Reversible capacity (mA h g <sup>-1</sup> ) | Capacity retention (%)/no. of cycles | Coulombic efficiency (%) | References  |
|---------|---|-----------|---------------------------------------|---|--------------------------------------|--------------------------|-------------|
| 1       | Fe-MIL-88B  | Anode     | 10                                    | 744.5                                       | 93/400                               | 100                      | 122         |
| 2       | Co <sub>2</sub> (OH) <sub>2</sub> BDC   | Anode     | 100                                   | 650   | —/100                                | 100                      | 123         |
| 3       | Co-BDC  | Anode     | 100                                   | 1090  | 70.7/1000                            | 99.46                    | 124         |
| 4       | S-Co-MOF  | Anode     | 200                                   | 1021  | —/200                                | 80.4                     | 101         |
| 5       | Co-COP  | Anode     | 200                                   | 573   | 100/1000                             | 100                      | 125         |
| 6       | Co-BTC  | Anode     | 100                                   | 750   | —/200                                | 79                       | 126         |
| 7       | Co-MOF  | Anode     | 100                                   | 400   | 84.2/80                              | 99.8                     | 127         |
| 8       | Co <sub>2</sub> (DOBDC)   | Anode     | 500                                   | 526.1                                       | —/200                                | 99                       | 128         |
| 9       | [Cu <sub>3</sub> (BTC) <sub>2</sub> ]   | Anode     | 96                                    | 474   | 100/50                               | 98                       | 129         |
| 10      | Mn-LCP  | Anode     | 390                                   | 390   | —/50                                 | —                        | 109         |
| 11      | Mn-BTC  | Anode     | 100                                   | 845   | 100/100                              | 97                       | 130         |
| 12      | Ni-MOF  | Anode     | 500                                   | 620   | —/200                                | 100                      | 131         |
| 13      | Zn <sub>3</sub> (HCOO) <sub>6</sub>   | Anode     | —                                     | 560   | —/200                                | —                        | 132         |
| 14      | [Pb(4,4'-ocppy) <sub>2</sub> ]·7H <sub>2</sub> O  | Anode     | 100                                   | 489   | 96/500                               | 98                       | 133         |
| 15      | Fe/Co-BTC   | Anode     | 1000                                  | 693.3                                       | —/600                                | 95                       | 134         |
| 16      | CoCGr-5   | Anode     | 1000                                  | 1368  | —/400                                | >99                      | 135         |
| 17      | Cu(2,7-AQDC)  | Cathode   | 105                                   | 105   | —/50                                 | —                        | 136         |
| 18      | Cd-HTTPCA   | Cathode   | 1000                                  | 200   | 22/200                               | 96.5                     | 137         |
| 19      | S@MOF-525(Cu)   | Cathode   | 250                                   | 700   | —/200                                | 100                      | 138         |
| 20      | Fe-MIL-101  | Cathode   | —                                     | 72  | —/100                                | 98                       | 139         |
| 21      | Fe-MIL-53   | Cathode   | 50                                    | 50  | —/50                                 | 80                       | 140         |
| 22      | Fe-MIL-68   | Cathode   | —                                     | 30  | —/3                                  | —                        | 141         |
| 23      | MOPOFS1   | Cathode   | —                                     | 68  | —/60                                 | 99                       | 142         |
| 24      | (Mn <sub>0.5</sub> )(Cu <sub>0.5</sub> )Fe-PBA  | Cathode   | 30                                    | 30  | —/50                                 | —                        | 143         |
| 25      | FeFe(CN) <sub>6</sub>   | Cathode   | 25                                    | 25  | —/50                                 | 99.6                     | 144         |
| 26      | MIL-47  | Cathode   | 10                                    | 10  | —/50                                 | —                        | 145         |
| 27      | Fe-MIL-101  | Cathode   | —                                     | 20  | —/30                                 | 79                       | 146 and 147 |
| 28      | Cd(ClO <sub>4</sub> ) <sub>2</sub> (DPNDI) <sub>2</sub>   | Cathode   | 100                                   | 100   | —/50                                 | 70                       | 148         |
| 29      | Fe-MIL-116  | Cathode   | —                                     | 72  | 40/100                               | 90                       | 149         |
| 30      | FeHCCo  | Cathode   | 200                                   | 116   | —/100                                | 99.6                     | 150         |
| 31      | Cu-TCA  | Cathode   | —                                     | 39.9  | 71.5/200                             | 96.5                     | 151         |
| 32      | Cu-CuPc   | Cathode   | —                                     | 151   | —/200                                | 95                       | 152         |
| 33      | Cu <sub>3</sub> (HHTP) <sub>2</sub>   | Cathode   | —                                     | 95  | 85/500                               | 100                      | 153         |
| 34      | Cu-THQ  | Cathode   | 500                                   | 50  | 85/100                               | 90                       | 154         |
| 35      | UiO-66  | Cathode   | —                                     | 38.8  | 65/30                                | —                        | 155         |
| 36      | Li <sub>2</sub> (VO) <sub>2</sub> (HPO <sub>4</sub> ) <sub>2</sub> (C <sub>2</sub> O <sub>4</sub> ) | Cathode   | 80                                    | 125   | —/25                                 | 97                       | 156         |
| 37      | Li-Co-BTC SNNU-73   | Cathode   | 50                                    | 155.6                                       | —/50                                 | 100                      | 157         |
| 38      | Li-Co-BTC SNNU-74   | Cathode   | 50                                    | 87.9  | —/50                                 | 100                      | 157         |

electrode materials also provide considerably good efficiency in lithium-ion batteries, so this advance opened a new avenue in the field of battery materials.<sup>94</sup> Compared to carbonaceous materials synthesized from conventional precursors, MOF-derived carbon materials have significant advantages of tailorable porosity, built-in functionalization, enhanced surface area and unique morphologies.<sup>74,95</sup>

The structural flexibility, efficient redox activity and affordable cost of MOF materials have made them good candidates for LIB electrodes. The high surface area and extent of porosity of such materials are beneficial for interfacial charge transport and to adapt to the strain developed due to lithium insertion/extraction. They also offer higher thermal stability. However, there are some associated shortcomings as well. The practical applications of many MOF structures are hampered by unsatisfactory cyclic performance due to the poor conductivity of the structure.<sup>6,96</sup> To overcome these problems, many modifications have been made in MOF and MOF-derived materials; like metal

doping and composite formation with carbonaceous materials. In this review, we have represented all such materials; pristine MOFs, MOF composites and MOF-derived compounds are evaluated as efficient electrode materials for lithium-ion batteries. We intend to cover as much of the data as possible to promote knowledge from previous studies for the sake of the generation of new ideas for next-generation LIBs.

## 2.2 Pristine MOF-based electrode materials for LIBs

The era of MOFs as electrodes for LIBs started back in 2007 when Ferey and co-workers introduced Fe-MIL-53 as an intercalation cathode material for rechargeable LIBs, but the reported capacity (75 mA h g<sup>-1</sup>) and cyclic stability were not very impressive.<sup>97</sup> Even so, it opened doors to a new way of research and development in the area of electrode chemistries for LIBs (Table 2). Later, Chowdhury *et al.*<sup>98</sup> performed the electrochemical analysis of Fe-MIL-53 and explained the redox activity



using density functional theory (DFT) and chemical bond analysis. Farisabadi *et al.* prepared Fe-MIL-101 by modifying the synthesis route.<sup>99</sup> In that study, it was found that the redox conversion of  $\text{Fe}^{2+}/\text{Fe}^{3+}$  was not perfectly reversible. Shen and co-workers studied another variation, Fe-MIL-88 with a functionalized carbonyl material.<sup>58</sup> The morphological and electrochemical analysis presented promising features. The material showed a capacity of  $86.8 \text{ mA h g}^{-1}$  over 100 cycles, proving that altering the synthesis route and controlling some physical parameters can lead to structural variations that are promising towards electrochemical improvements.

Another option in this run is the use of cobalt instead of iron. Hu and co-workers prepared Co-MOF anode material by a one-pot synthesis route. The material showed a high capacity of  $1090 \text{ mA h g}^{-1}$  and better cyclic stability.<sup>100</sup> Another alternative was a shell-like S-Co-MOF that was prepared by a solvothermal process.<sup>101</sup> It also showed good cyclic stability, but the lithium-ion storage capacity was not good. Song *et al.*<sup>102</sup> prepared the same one-dimensional material Co-MOF through a hydrothermal method known as co-coordination polymer nanowires which showed  $1100 \text{ mA h g}^{-1}$ .<sup>103</sup> Later on, Li *et al.*<sup>104</sup> produced Co-based copolymers with different morphologies. These products retained a capacity of  $47 \text{ mA h g}^{-1}$  after 500 cycles and maintained almost 100% coulombic efficiency.<sup>105,106</sup> Research on these materials for electrode applications also paved the way for other metal alternatives. Later, these MOF structures were also prepared using Cu, Ni and Mn metallic centers. The redox-active sites in all these compounds were obtained *via* a special synthetic strategy. The best example to discuss here is Cu-MOF with an anthraquinone<sup>107,108</sup> based organic linker. The organic units attach to the Cu center and make a zig-zag arrangement inside the 2D layers. There are weak pi-pi linkages between the layers. On using the same material as an electrode for a lithium-ion battery with a controlled voltage window, a very high cyclic reproducibility was achieved. Another Cu-MOF was prepared with tricarboxytriphenyl amine (Cu-TCA). It was also tested

as a cathode material and just like the other Cu-MOFs, it also showed an excellent cyclic stability and rate performance.

Liu and his co-workers<sup>109</sup> prepared Mn-MOFs with different organic linkers by adopting different reaction schemes. Mn-MOF with tetrafluoroterephthalic acid was tested for lithium batteries but the lithium storage capacity was not up to the mark. To improve this capacity, 1,3,5-benzene tricarboxylate was tested as an organic linker by Maiti *et al.*<sup>110,111</sup> which offered better electrochemical properties as an anode for LIBs. The chemistry behind these electrochemical properties mainly involves pi-pi interactions inside the aromatic part of the organic linker. The conjugation present inside the benzene ring stabilizes the three-dimensional structure of the MOF. Later, a new concept of a bipolar charge mechanism was introduced by Zhang and his co-workers.<sup>112,113</sup> They first tested Mn-MOFs with quinone as the organic linker as an active cathode material and then introduced a series of modifications by replacing Mn with a trivalent metallic cation and replacing quinone with electron-donor organic linkers.<sup>114-117</sup> This modification offered greater discharge voltage and higher energy density. Later on, a series of experiments were performed by various scientists to understand the electrochemical behavior of different metals in LIBs. Tian *et al.* tested Cd-MOF and Co-MOF for this purpose.<sup>118-121</sup> They prepared metallic MOF samples with variable anion and thermodynamic control and tested them for LIBs. Cd-MOFs performed better than Co-MOFs. The characterization analysis showed that the electrochemical behavior is greatly affected by metallic nodes and the level of porosity achieved during fabrication.

Saravanan *et al.* tested the electrochemical performance of Zn MOFs for LIBs.<sup>158</sup> They prepared a series of samples with the metals Zn and Co in ratios of 1 : 0, 0 : 1 and 1 : 1. The sample with Zn metal and without Co mixing showed the best results. The cyclic stability of bimetallic samples with Co in a particular proportion was also good, but not up to the mark. The lithium storage mechanism involved the formation of lithium formate



Fig. 11 Mechanism involving the formation of lithium formate (FOR) structures during charging and discharging cycles. Reproduced from ref. 158 with permission from Royal Society of Chemistry, Copyright 2010.



(Fig. 11), as depicted by the *ex situ* FTIR results, rather than the typically formed lithium oxide.

Kaveevitchai and co-workers prepared MOFs of vanadium with benzene dicarboxylic acid (BDC) (MIL-47) and tested them for use in LIBs.<sup>145</sup> They exhibited excellent capacity performance (82 mA h g<sup>-1</sup>) which was even greater than that of MIL-53 (Fe) at C/12.<sup>159</sup> Another alternative turned out to be UiO-66 as a Zr MOF with 12 extension points of BDC synthesized by reducing the reaction temperature. During the process of lithiation and delithiation in UiO-66, much less volume change was observed, as interpreted by the consistent XRD patterns of both lithiated and delithiated electrode materials.

MOFs with better thermal and chemical stability were prepared by using various synthesis strategies. MOFs with hydrophobic and polar properties were synthesized and tested for use in LIBs. All these materials showed stable and reproducible electrochemical results. The porosity level also played a significant role in lithium storage and transportation. Ogihara *et al.* prepared an intercalated metal-organic framework (iMOF) for high-voltage bipolar batteries.<sup>160</sup> The greatest advantage achieved in this structure was that during the intercalation process the architecture of the iMOF remained intact, which facilitated lithium transportation giving rise to favorable cyclic stability.

Some metals showed better cyclic stability while others provided high energy density and enhanced capacity. The eagerness to achieve a single electrode structure with all these required characteristics made scientists prepare and study bimetallic MOF structures. These structures provided a synchronised effect of all the electrochemical features both the metals had for LIBs. For example, Xu *et al.* prepared Co-Fe-BTC nanotubes *via* a solvothermal process.<sup>161</sup> Similarly, Mn-BTC MOFs have poor cyclic stability. Zhang and his co-workers prepared a bimetallic Co-Mn-BTC MOF structure and achieved a high capacity of 901 mA h g<sup>-1</sup> after 150 cycles.<sup>162</sup> Liu *et al.*<sup>163</sup> introduced the idea of using MOFs and their molecular structures as separators for the coin cell fabrication of LIBs. They used a nitrogen-doped titania MOF (Ti-MIL-125) coated separator in an LIB half-cell.<sup>164,165</sup> This facilitated dendritic-free lithium deposition and long-term, easy and reversible lithium stripping and opened ways to study how to protect the lithium anode using MOF structures.

In solid-state LIBs, MOFs are not just tested as an electrode material but also as an alternative electrolyte.<sup>166</sup> Angulakshami *et al.* prepared a MOF with Mg as the metallic center and benzene tricarboxylic acid (Mg-BTC-MOFs) and embedded it in a polymeric matrix to use it as a solid-state electrolyte for LIBs.<sup>167</sup> The material showed a dramatic increase in thermal stability compared to the usual electrolyte, proving itself to be compatible with lithium transport. The material also showed an elongation at break factor comparable to the pure polymeric matrix.

### 2.3. MOF-based composites as electrode materials for LIBs

The idea of composite formation came to the fore for improving the conductivity of electrode materials containing MOFs. Generally, a MOF structure is a porous entity that provides

ample space for ionic/atomic storage. As far as conductivity is concerned, MOFs could not provide promising conductive properties. To achieve better conductivity, composites of MOFs with exclusively conductive materials were made.<sup>168</sup> Examples include metal oxides, conductive polymers, conductive metals, carbon materials, and nanomaterials. Nanocomposites in particular offered better cyclic stability and enhanced capacity when tested as anode materials for LIBs. Han *et al.* introduced a new MOF sandwich coating (MOF-SC) method for preparing MOF composites.<sup>169</sup> The idea was to use a MOF layer as a protective cushion for efficient silicon-based anodes, providing a more stable structure and enhanced electrochemical features. For example, a micro silicon MOF sandwich structure (C-Si-ZIF-8) exhibited 1700  $\mu\text{A h cm}^{-2}$  of areal capacity. The better performance is attributed to the fact that a MOF layer with larger pores and a larger surface area can accommodate more electrolyte and provide faster and better lithium diffusion. Also, this sandwich structure is easy to operate, which makes it promising for future industrial applications. Using this method, they prepared MOF composites with various MOF structures: *e.g.*, MOF-5, HKUST-1, MIL-53, N-doped-MIL-53, and ZIF-67. Dong *et al.* prepared Co and Cd MOFs and their composites with reduced graphene oxide (rGO). An analysis of electrochemical performance showed that the rGO composite with MOF had retained a discharge capacity of 500 mA g<sup>-1</sup> after 120 cycles.<sup>170,171</sup> After the promising result of an rGO composite with MOF, the scientists tried composites with other nano-alternatives. For example, an Ni MOF composite with CNTs displayed better performance and enhanced activity in LIBs as compared to the pristine Ni<sub>3</sub>(-HOOC)<sub>6</sub> MOF.<sup>41</sup>

MOF composites were also tested as electrolyte material for solid-state LIBs. Gerbaldi and co-workers presented the excellent dispersion of Al-BTC MOF in a polyethylene oxide matrix as an electrolyte for LIBs.<sup>172</sup> The as-prepared MOF-nanocomposite polymeric electrolyte (NCPE) showed stable lithium storage even after an extended storage time. Ionic liquid impregnated MOF nanocrystals were also tested as electrolytes for LIBs. The idea was first introduced by Wang and his team. Later on, this idea was extended to other battery systems like sodium-ion, potassium-ion and aluminum-ion batteries.<sup>173</sup> All of them displayed promising energy storage and effective transport phenomena. Despite noticeable progress, the insulating properties of MOFs prevent them achieving the required level of stability for lithium intercalation. Under actual operating conditions, there is still a lot of room for improvement in cyclic stability, capacity and energy density to be achieved along with the basic features of long cyclic life and low cost.

### 2.4. MOF-derived metal oxide composite based electrode material for LIBs

MOFs are a series of crystalline porous structures originating from metal salt precursors and organic linkers. Thus, pyrolyzing the MOF structures at a favorable temperature in an inert environment can take them back to the oxide of metals used in them with nanosized structures. Not only that, but pyrolysis



Table 3 MOF-derived metal oxide–carbon composite anode materials for lithium-ion batteries

| Sr. no. | Electrode material                                 | MOF template                                     | Current Electrode density (mA g <sup>-1</sup> ) | Reversible capacity (mAh g <sup>-1</sup> ) | Capacity retention/ number of cycles | Coulombic efficiency | Reference   |
|---------|--|--|---|--|--------------------------------------|----------------------|-------------|
| 1       | Fe <sub>3</sub> O <sub>4</sub> /C                  | Fe-MOFs  | Anode 100                                       | 975  | 70/50                                | 100                  | 188–190     |
| 2       | LFP/N-CNWs   | Fe-MIL-100                                       | Cathode 67.5                                    | 161.5                                      | 70.9/–                               | 94.3                 | 191         |
| 3       | NG/Fe–Fe <sub>3</sub> C                            | Fe-MIL-100                                       | Anode 100                                       | 1098                                       | —/48                                 | 96.2                 | 192         |
| 4       | Co <sub>3</sub> O <sub>4</sub> /Co/carbon          | ZIF-67   | Anode 100                                       | 850  | 90/60                                | 75                   | 193         |
| 5       | MWCNTs/Co <sub>3</sub> O <sub>4</sub>              | MWCNTs/ZIF-67                                    | Anode 100                                       | 813  | —/100                                | 95                   | 194         |
| 6       | ZnO@ZnO QDs/C NRAs                                 | ZnO@ZIF-8 NRAs                                   | Anode 100                                       | 1055                                       | 89/100                               | 99.8                 | 195         |
| 7       | C–ZnCo <sub>2</sub> O <sub>4</sub> –ZnO NRAs       | ZIF-8–ZnCo <sub>2</sub> O <sub>4</sub> –ZnO NRAs | Anode 200                                       | 1318                                       | —/150                                | —                    | 196         |
| 8       | ZnS NR@HCP   | ZIF-8  | Anode 600                                       | 840  | 76/300                               | 98                   | 197         |
| 9       | SnO <sub>2</sub> @C                                | SnO <sub>2</sub> @ZIF-8                          | Anode 100                                       | 1032                                       | 96/100                               | 99                   | 198–200     |
| 10      | Sn@C   | Sn-MOF   | Cathode 200                                     | 1081                                       | 80/100                               | 99.7                 | 201 and 202 |
| 11      | SnO <sub>2</sub> @N-RGO                            | Sn-MOF   | Anode 200                                       | 1041                                       | 76.4/180                             | 100                  | 203         |
| 12      | Sn-NPC   | Sn-MOF   | Anode 200                                       | 740  | 85/200                               | 89                   | 204         |
| 13      | Li <sub>4</sub> Ti <sub>5</sub> O <sub>12</sub> /C | Li-doped Ti-MOF                                  | Anode 500                                       | 128.8                                      | 96.8/50                              | —                    | 205–207     |
| 14      | TiO <sub>2</sub> /C                                | Ti-MIL-125                                       | Anode 500                                       | 114.2                                      | —/200                                | 99                   | 208 and 209 |
| 15      | MnO@C  | Mn-BTC   | Anode 150                                       | 470  | 90/50                                | 60.8                 | 210         |
| 16      | In <sub>2</sub> O <sub>3</sub> /C                  | In-MOF   | Anode 100                                       | 869  | —/100                                | 58.4                 | 211         |
| 17      | NiSb-CHSs  | Ni-MOF   | Anode 100                                       | 497.3                                      | —/100                                | 98                   | 212         |
| 18      | N modified carbon                                  | Cu-MOFs  | Anode 100                                       | 409  | 99/50                                | 99                   | 213 and 214 |
| 19      | TiN/NC   | Ti-MIL-125                                       | Anode 400                                       | 1024                                       | 85/550                               | 84.7                 | 215         |
| 20      | 3D PC  | MOF-5  | Anode 200                                       | 849  | 99/200                               | 99                   | 216         |

also develops a nanoporous carbon matrix derived from organic ligands in which these nanosized metal oxide structures are embedded. In other words, this is a direct method of preparing an *in situ* MO/C nanocomposite using MOF as a template or precursor (Table 3). Li *et al.*<sup>174</sup> prepared an Fe<sub>3</sub>O<sub>4</sub>/C microcuboid composite using Fe-MOF (Fe-(OOC)<sub>2</sub>)<sub>2</sub>·2H<sub>2</sub>O. by heating it at 400 °C for 2 hours in an inert atmosphere. The as-synthesized composite showed stable cyclic behavior and great rate capability. Chen *et al.*<sup>175</sup> repeated the same process with a little modification. They directly carbonized the Fe-MOF (Fe-BDC) under the above given conditions. The obtained nano-architecture of Fe<sub>3</sub>O<sub>4</sub>/C exhibited a lithium storage capacity of 861 mA g<sup>-1</sup> after 100 cycles. Similar types of metal oxide nanocomposite with porous carbon (MO/C) with desirable features and electrochemical behavior were prepared by a facile method introduced by Zheng *et al.*<sup>176,177</sup> They synthesized ultrasmall MnO nanostructures embedded homogeneously in a nanoporous carbon matrix which showed 1221 mA h g<sup>-1</sup> of capacity at the 100<sup>th</sup> cycle.<sup>178</sup> Wang and co-workers prepared a TiO<sub>2</sub>/C composite by two-step calcination of Ti-MIL-125.<sup>179,180</sup> The two-step calcination enables the development of sub-micrometer tablet-type structures of a titania oxide–carbon composite which presented a highly reversible capacity of 1000 mA h g<sup>-1</sup> and greater rate capability.

In the process of finding better and easier ways of synthesizing these metal oxide–C composites, scientists tried and tested many synthetic routes under various synthesis conditions. Shen *et al.* meanwhile offered a way of directly preparing ZnO quantum dots/C core–shell nanorod arrays.<sup>181</sup> The process

was performed over a carbon cloth substrate *via* a scalable *in situ* ion exchange method. First, ZnO nanorods were prepared over the carbon cloth and then these prepared ZnO nanorods were used as a template for making ZnO@ZIF-67 nanorods<sup>182,183</sup> which were then annealed at high temperature in an inert atmosphere. The synthesized material was smaller in diameter, providing a larger surface area, and was fluffy in texture. Another technique was introduced by Huang *et al.* in which they synthesized *in situ* composite ZIF-67/MWCNTs by using a Co precursor and 2-methylimidazole in the presence of MWCNTs.<sup>184</sup> Later, this composite was annealed at high temperature in an argon environment to achieve a CoO/C nanocomposite. The material provided a smooth surface with greater area and 500 nm size. The material showed a rate capacity of 813 mA h g<sup>-1</sup> after 100 cycles. The same scheme was also followed by the scientists to prepare a bimetallic nanocomposite with MWCNTs using bimetallic MOF structures: for example, Co and Fe.<sup>185,186</sup> The morphologies for both samples were the same. The rate capacity was even better due to the enhanced conductivity. Following this synthesis strategy, Jin *et al.*<sup>187</sup> prepared an InO/C composite from In-MOF and tested it as an anode for LIBs. The cyclic performance was very good as it exhibited a reversible discharge capacity of 720 mA h g<sup>-1</sup> after 150 cycles.

Compared to the composites with a single metal oxide, those with bimetallic oxides offered better cyclic stability. Due to the low activation energy required for electron transfer, the bimetallic oxide–carbon composite offered a greater rate capability with lithiation and delithiation processes. Wu *et al.* tested the



same feature with Cu–Co<sub>2</sub>O<sub>4</sub> coated with carbon nanolayers.<sup>217</sup> The material exhibited a discharge capacity of 750 mA h g<sup>-1</sup> after 50 cycles. Similarly, Tang *et al.* tested lithiated titania MOF pyrolyzed to Li<sub>4</sub>Ti<sub>5</sub>O<sub>12</sub>-C (LTO/C)<sup>218</sup> and Yong *et al.* grew a ZnO/C nanorod array on tin foil as the substrate.<sup>219</sup> Both samples were tested as anodes for LIBs. Both represented a rate capacity of more than 1300 mA h g<sup>-1</sup> after 150 cycles with a great rate capability.

### 2.5. MOF derived metal nanoparticle composites as electrode material for LIBs

The conductive nature of metals and the large surface area offered by nanocomposites fascinated a lot of researchers for their energy-related applications, especially as electrodes for LIBs. Shiva *et al.*<sup>220,221</sup> developed a direct synthesis route by the carbonization of Sn-based MOFs to achieve Sn nanoparticles embedded in a carbon matrix. The NSn@C anode material showed a considerably high specific capacitance of 1225 mA h g<sup>-1</sup> with 60% coulombic efficiency. Similarly, Ni-MOF was prepared by Yu *et al.*<sup>222</sup> which was then modified by the addition of Sb metal and this material was then pyrolyzed to Ni-Sb nanoparticles in a carbon matrix. The alloy nanomaterial offered a discharge capacity of 497.3 mA h g<sup>-1</sup> after 100 cycles with 58% coulombic efficiency.<sup>223,224</sup>

## 3. Conclusions

A number of carbon and metal based materials that have been prepared and tested as electrodes for LIBs have been reviewed. Over the course of many years, research and development have focused mainly on finding feasible and cheaper methods to develop materials with controllable morphologies and assemblies. The synthesis of porous, hollow and unique core-shell architectures derived from metal-organic frameworks represented promising electrochemical performance in lithium-ion batteries. Playing with the structural features of MOFs and materials derived from them by controlling the temperature and other reaction conditions has given rise to many remarkable electrode materials, not just for LIBs but also for many other battery chemistries. The overall comparison of all the material types mentioned in this study shows that the incorporation of a nanomaterial as a composite with MOF or a nanomaterial derived from MOF show enhanced electrochemical behavior by providing a greater surface area and a higher level of porosity. As far as conductivity is concerned, metals with better conductivity used in pristine MOFs and metal alloys derived from bimetallic MOFs with hollow porous structures solved the problem of poor conductivity of MOFs in lithium-ion batteries. All these variations offered sufficient cyclic stability, conductivity, structural stability, a shorter lithium diffusion distance, more lithium storage space and enhanced electron uptake efficiency. Therefore, all these have offered considerably good rate capacities and coulombic efficiencies. Thus, they opened ways for their implementation in other energy applications and industrial trials as well. Further research in metal-organic framework should tend to aim at

better chemical stability in the structure with improved kinetics in various energy applications.

## 4. Future perspectives

The review presented here represents not just the strength of metal-organic framework based electrode materials for battery development but also points to the fact that the cyclic stability of a lithium-ion battery with a MOF as the electrode counterpart, although growing, still needs a great deal of research and development. For the sake of bringing MOF-based battery set-ups to the level of commercialization, research and development in improving the cyclic stability of these electrode-based materials is the need of the hour. A lot of important strategies can be adopted in this regard. For instance, making composite structures of MOFs with nanomaterials or deriving unique nanoarchitectures from MOFs with carefully optimized reaction conditions to control three-dimensional morphologies. Similarly, the incorporation of highly conductive transition metal within the structure through core-shell methods can also play an important role in bringing about efficient MOF-based electrode materials for lithium-ion batteries. Moreover, constant collaboration between scientific research and industry is required to achieve the commercialization of MOF-based electrode materials for lithium-ion batteries. Based on a comparison of different structural modifications for the purpose of obtaining a better charging-discharging capacity, it is quite evident that nano-activated and derived carbon structures perform quite well. Therefore, to further improve the performance of MOF-based electrode materials, the best strategy is to switch to a focus on hybrid structures where one can benefit from the synergistic effect of the highly porous framework of carbon and the highly conductive metal oxide network for better cyclic life and delayed aging of the batteries.

## Conflicts of interest

There are no conflicts to declare.

## References

- 1 B. Scrosati, History of lithium batteries, *J. Solid State Electrochem.*, 2011, **15**(7–8), 1623–1630.
- 2 T. Kim, W. Song, D.-Y. Son, L. K. Ono and Y. Qi, Lithium-ion batteries: outlook on present, future, and hybridized technologies, *J. Mater. Chem. A*, 2019, **7**(7), 2942–2964.
- 3 R. Borah, F. Hughson, J. Johnston and T. Nann, On battery materials and methods, *Mater. Today Adv.*, 2020, **6**, 100046.
- 4 A. Vu, Y. Qian and A. Stein, Porous Electrode Materials for Lithium-Ion Batteries—How to Prepare Them and What Makes Them Special, *Adv. Energy Mater.*, 2012, **2**(9), 1056–1085.
- 5 V. Chabot, S. Farhad, Z. Chen, A. S. Fung, A. Yu and F. Hamdullahpur, Effect of electrode physical and chemical properties on lithium-ion battery performance, *Int. J. Energy Res.*, 2013, **37**(14), 1723–1736.
- 6 G. Zhang, L. Jin, R. Zhang, Y. Bai, R. Zhu and H. Pang, Recent advances in the development of electronically and



- ionically conductive metal-organic frameworks, *Coord. Chem. Rev.*, 2021, **439**, 213915.
- 7 G. J. Boink, V. M. Christoffels, R. B. Robinson and H. L. Tan, The past, present, and future of pacemaker therapies, *Trends Cardiovasc. Med.*, 2015, **25**, 661–673.
  - 8 B. Scrosati, K. Abraham, W. A. van Schalkwijk, and J. Hassoun, *Lithium batteries: advanced technologies and applications*. John Wiley & Sons, 2013.
  - 9 K. Xu, Nonaqueous liquid electrolytes for lithium-based rechargeable batteries, *Chem. Rev.*, 2004, **104**(10), 4303–4418.
  - 10 W. Chen, *et al.*, Designing Safe Electrolyte Systems for a High-Stability Lithium–Sulfur Battery, *Adv. Energy Mater.*, 2018, **8**(10), 1702348.
  - 11 L. Zhang, *et al.*, Platinum-based nanocages with subnanometer-thick walls and well-defined, controllable facets, *Science*, 2015, **349**(6246), 412–416.
  - 12 Y. Wang, Q. Sun, Q. Zhao, J. Cao and S. Ye, Rechargeable lithium/iodine battery with superior high-rate capability by using iodine–carbon composite as cathode, *Energy Environ. Sci.*, 2011, **4**(10), 3947–3950.
  - 13 W. Greatbatch and C. F. Holmes, The lithium/iodine battery: a historical perspective, *Pacing Clin. Electrophysiol.*, 1992, **15**(11), 2034–2036.
  - 14 R. Gangadharan, P. Namboodiri, K. Prasad and R. Viswanathan, The lithium–thionyl chloride battery—a review, *J. Power Sources*, 1979, **4**(1), 1–9.
  - 15 D. Lisbona and T. Snee, A review of hazards associated with primary lithium and lithium-ion batteries, *Process Saf. Environ. Prot.*, 2011, **89**(6), 434–442.
  - 16 H. Kim, *et al.*, Exploiting Lithium–Ether Co-Intercalation in Graphite for High-Power Lithium-Ion Batteries, *Adv. Energy Mater.*, 2017, **7**(19), 1700418.
  - 17 Z. Shu, R. McMillan and J. Murray, Electrochemical intercalation of lithium into graphite, *J. Electrochem. Soc.*, 1993, **140**(4), 922.
  - 18 M. S. Whittingham, Ultimate limits to intercalation reactions for lithium batteries, *Chem. Rev.*, 2014, **114**(23), 11414–11443.
  - 19 N. Imanishi, M. Toyoda, Y. Takeda and O. Yamamoto, Study on lithium intercalation into MoS<sub>2</sub>, *Solid State Ionics*, 1992, **58**(3–4), 333–338.
  - 20 P. B. Balbuena and Y. Wang, *Lithium-ion batteries: solid-electrolyte interphase*, Imperial College Press, 2004.
  - 21 J. Li, C. Ma, M. Chi, C. Liang and N. J. Dudney, Solid electrolyte: the key for high-voltage lithium batteries, *Adv. Energy Mater.*, 2015, **5**(4), 1401408.
  - 22 Y. Zhu, X. He and Y. Mo, Origin of outstanding stability in the lithium solid electrolyte materials: insights from thermodynamic analyses based on first-principles calculations, *ACS Appl. Mater. Interfaces*, 2015, **7**(42), 23685–23693.
  - 23 B. Scrosati, Lithium rocking chair batteries: an old concept?, *J. Electrochem. Soc.*, 1992, **139**(10), 2776.
  - 24 S. H. Lee, P. Liu, C. E. Tracy and D. K. Benson, All-Solid-State Rocking Chair Lithium Battery on a Flexible Al Substrate, *Electrochem. Solid-State Lett.*, 1999, **2**(9), 425.
  - 25 B. Scrosati, Recent advances in lithium ion battery materials, *Electrochim. Acta*, 2000, **45**(15–16), 2461–2466.
  - 26 B. Wang, J. Bates, F. Hart, B. Sales, R. Zuhr and J. Robertson, Characterization of thin-film rechargeable lithium batteries with lithium cobalt oxide cathodes, *J. Electrochem. Soc.*, 1996, **143**(10), 3203.
  - 27 P. He, H. Yu and H. Zhou, Layered lithium transition metal oxide cathodes towards high energy lithium-ion batteries, *J. Mater. Chem.*, 2012, **22**(9), 3680–3695.
  - 28 P. Calandra, G. Calogero, A. Sinopoli and P. G. Gucciardi, Metal nanoparticles and carbon-based nanostructures as advanced materials for cathode application in dye-sensitized solar cells, *Int. J. Photoenergy*, 2010, **2010**, 109495.
  - 29 W.-J. Zhang, A review of the electrochemical performance of alloy anodes for lithium-ion batteries, *J. Power Sources*, 2011, **196**(1), 13–24.
  - 30 C. Julien and Z. Stoyanov, *Materials for Lithium-Ion Batteries*, Springer Netherlands, 2012.
  - 31 X. Shen, H. Liu, X.-B. Cheng, C. Yan and J.-Q. Huang, Beyond lithium ion batteries: higher energy density battery systems based on lithium metal anodes, *Energy Storage Mater.*, 2018, **12**, 161–175.
  - 32 O. M. Yaghi, G. Li and H. Li, Selective binding and removal of guests in a microporous metal–organic framework, *Nature*, 1995, **378**(6558), 703–706.
  - 33 F. Zafar and E. Sharmin, *Metal-Organic Frameworks*, IntechOpen, 2016.
  - 34 H. Wang, Q.-L. Zhu, R. Zou and Q. Xu, Metal-organic frameworks for energy applications, *Chem*, 2017, **2**(1), 52–80.
  - 35 A. Indra, T. Song and U. Paik, Metal organic framework derived materials: progress and prospects for the energy conversion and storage, *Adv. Mater.*, 2018, **30**(39), 1705146.
  - 36 L. R. MacGillivray, *Metal-Organic Frameworks: Design and Application*, Wiley, 2010.
  - 37 L. R. MacGillivray and C. M. Lukehart, *Metal-Organic Framework Materials*, Wiley, 2014.
  - 38 C. Weinberger and M. Tiemann, *Functional Nanoporous Materials*, MDPI AG, 2020.
  - 39 M. H. Yap, K. L. Fow and G. Z. Chen, Synthesis and applications of MOF-derived porous nanostructures, *Green Energy Environ.*, 2017, **2**(3), 218–245.
  - 40 A. Kirchon, L. Feng, H. F. Drake, E. A. Joseph and H.-C. Zhou, From fundamentals to applications: a toolbox for robust and multifunctional MOF materials, *Chem. Soc. Rev.*, 2018, **47**(23), 8611–8638.
  - 41 T. Noor, N. Zaman, H. Nasir, N. Iqbal and Z. Hussain, Electro catalytic study of NiO-MOF/rGO composites for methanol oxidation reaction, *Electrochim. Acta*, 2019, **307**, 1–12.
  - 42 S. Hanif, X. Shi, N. Iqbal, T. Noor, R. Anwar and A. Kannan, ZIF derived PtNiCo/NC cathode catalyst for proton exchange membrane fuel cell, *Appl. Catal., B*, 2019, **258**, 117947.
  - 43 L. Yaqoob, *et al.*, Nanocomposites of cobalt benzene tricarboxylic acid MOF with rGO: an efficient and robust electrocatalyst for oxygen evolution reaction (OER), *Renewable Energy*, 2020, **156**, 1040–1054.
  - 44 L. Yaqoob, T. Noor, N. Iqbal, H. Nasir and N. Zaman, Development of nickel-BTC-MOF-derived nanocomposites with rGO towards electrocatalytic oxidation of methanol and its product analysis, *Catalysts*, 2019, **9**(10), 856.



- 45 T. Noor, M. Ammad, N. Zaman, N. Iqbal, L. Yaqoob and H. Nasir, A highly efficient and stable copper BTC metal organic framework derived electrocatalyst for oxidation of methanol in DMFC application, *Catal. Lett.*, 2019, **149**(12), 3312–3327.
- 46 E. Sarwar, T. Noor, N. Iqbal, Y. Mehmood, S. Ahmed and R. Mehek, Effect of Co-Ni Ratio in Graphene Based Bimetallic Electro-catalyst for Methanol Oxidation, *Fuel cells*, 2018, **18**(2), 189–194.
- 47 A. Asghar, *et al.*, Ethylenediamine loading into a manganese-based metal-organic framework enhances water stability and carbon dioxide uptake of the framework, *R. Soc. Open Sci.*, 2020, **7**(3), 191934.
- 48 Y.-Q. Lan, *et al.*, A Well-Defined Dual Mn-Sites based Metal-Organic Framework to Promote CO<sub>2</sub> Reduction/Evolution in Li-CO<sub>2</sub> Batteries, *Chem. Commun.*, 2021, DOI: 10.1039/D1CC03431F.
- 49 N. Zaman, T. Noor and N. Iqbal, Recent advances in the metal-organic framework-based electrocatalysts for the hydrogen evolution reaction in water splitting: a review, *RSC Adv.*, 2021, **11**(36), 21904–21925.
- 50 R. Cui, P. Zhao, Y. Yan, G. Bao, A. Damirin and Z. Liu, Outstanding Drug-Loading/Release Capacity of Hollow Fe-Metal-Organic Framework-Based Microcapsules: A Potential Multifunctional Drug-Delivery Platform, *Inorg. Chem.*, 2021, **60**(3), 1664–1671.
- 51 O. Shekhah, J. Liu, R. Fischer and C. Wöll, MOF thin films: existing and future applications, *Chem. Soc. Rev.*, 2011, **40**(2), 1081–1106.
- 52 J. Yu, *et al.*, Nanoparticle/MOF composites: preparations and applications, *Mater. Horiz.*, 2017, **4**(4), 557–569.
- 53 X. Lian, *et al.*, Enzyme-MOF (metal-organic framework) composites, *Chem. Soc. Rev.*, 2017, **46**(11), 3386–3401.
- 54 Z.-Y. Sui, P.-Y. Zhang, M.-Y. Xu, Y.-W. Liu, Z.-X. Wei and B.-H. Han, Metal-organic framework-derived metal oxide embedded in nitrogen-doped graphene network for high-performance lithium-ion batteries, *ACS Appl. Mater. Interfaces*, 2017, **9**(49), 43171–43178.
- 55 X. Li, M. R. Hill, H. Wang and H. Zhang, Metal-Organic Framework-Based Ion-Selective Membranes, *Adv. Mater. Technol.*, 2021, 2000790.
- 56 X. Li, *et al.*, Metal-Organic Framework-Derived Carbons for Battery Applications, *Adv. Energy Mater.*, 2018, **8**(23), 1800716.
- 57 G. Zou, *et al.*, Metal-organic framework-derived materials for sodium energy storage, *Small*, 2018, **14**(3), 1702648.
- 58 L. Shen, H. Song and C. Wang, Metal-organic frameworks triggered high-efficiency Li storage in Fe-based polyhedral nanorods for lithium-ion batteries, *Electrochim. Acta*, 2017, **235**, 595–603.
- 59 W. Shi, X. Xu, L. Zhang, W. Liu and X. Cao, Metal-organic framework-derived structures for next-generation rechargeable batteries, *Funct. Mater. Lett.*, 2018, **11**(6), 1830006.
- 60 C. Wang, *et al.*, Metal-organic framework-derived one-dimensional porous or hollow carbon-based nanofibers for energy storage and conversion, *Mater. Horiz.*, 2018, **5**(3), 394–407.
- 61 R. R. Salunkhe, Y. V. Kaneti and Y. Yamauchi, Metal-Organic Framework-Derived Nanoporous Metal Oxides toward Supercapacitor Applications: Progress and Prospects, *ACS Nano*, 2017, **11**(6), 5293–5308.
- 62 N. Stock and S. Biswas, Synthesis of metal-organic frameworks (MOFs): routes to various MOF topologies, morphologies, and composites, *Chem. Rev.*, 2012, **112**(2), 933–969.
- 63 N. A. Khan and S. H. Jhung, Synthesis of metal-organic frameworks (MOFs) with microwave or ultrasound: Rapid reaction, phase-selectivity, and size reduction, *Coord. Chem. Rev.*, 2015, **285**, 11–23.
- 64 Z. Li and L. Yin, Nitrogen-doped MOF-derived micropores carbon as immobilizer for small sulfur molecules as a cathode for lithium sulfur batteries with excellent electrochemical performance, *ACS Appl. Mater. Interfaces*, 2015, **7**(7), 4029–4038.
- 65 Z. Li, B. Li, L. Yin and Y. Qi, Prussian blue-supported annealing chemical reaction route synthesized double-shelled Fe<sub>2</sub>O<sub>3</sub>/Co<sub>3</sub>O<sub>4</sub> hollow microcubes as anode materials for lithium-ion battery, *ACS Appl. Mater. Interfaces*, 2014, **6**(11), 8098–8107.
- 66 G. Huang, L. Zhang, F. Zhang and L. Wang, Metal-organic framework derived Fe<sub>2</sub>O<sub>3</sub>@NiCo<sub>2</sub>O<sub>4</sub> porous nanocages as anode materials for Li-ion batteries, *Nanoscale*, 2014, **6**(10), 5509–5515.
- 67 F. Zou, *et al.*, MOF-derived porous ZnO/ZnFe<sub>2</sub>O<sub>4</sub>/C octahedra with hollow interiors for high-rate lithium-ion batteries, *Adv. Mater.*, 2014, **26**(38), 6622–6628.
- 68 L. Hou, L. Lian, L. Zhang, G. Pang, C. Yuan and X. Zhang, Self-sacrifice template fabrication of hierarchical mesoporous Bi-Component-Active ZnO/ZnFe<sub>2</sub>O<sub>4</sub> sub-microcubes as superior anode towards high-performance lithium-ion battery, *Adv. Funct. Mater.*, 2015, **25**(2), 238–246.
- 69 X. Ge, Z. Li, C. Wang and L. Yin, Metal-Organic Frameworks Derived Porous Core/Shell Structured ZnO/ZnCo<sub>2</sub>O<sub>4</sub>/C Hybrids as Anodes for High-Performance Lithium-Ion Battery, *ACS Appl. Mater. Interfaces*, 2015, **7**(48), 26633–26642.
- 70 J. Tang and Y. Yamauchi, Carbon materials: MOF morphologies in control, *Nat. Chem.*, 2016, **8**(7), 638–639.
- 71 S. Kaskel, *The Chemistry of Metal-Organic Frameworks*, 2 Volume Set: Synthesis, Characterization, and Applications, Wiley, 2016, vol. 1.
- 72 K. K. Gangu, S. Maddila, S. B. Mukkamala and S. B. Jonnalagadda, Characteristics of MOF, MWCNT and graphene containing materials for hydrogen storage: A review, *J. Energy Chem.*, 2019, **30**, 132–144.
- 73 P. Silva, S. Vilela, J. Tomé and F. Paz, Multifunctional metal-organic frameworks: From academia to industrial applications, *Chem. Soc. Rev.*, 2015, **44**, 6774–6803.
- 74 Z. Liang, R. Zhao, T. Qiu, R. Zou and Q. Xu, Metal-organic framework-derived materials for electrochemical energy applications, *EnergyChem*, 2019, **1**(1), 100001.
- 75 M. Peng, *et al.*, Oxidation of Ethylbenzene Using Nickel Oxide Supported Metal Organic Framework Catalyst, *Bull. Korean Chem. Soc.*, 2014, **35**, 3213–3218.



- 76 R. Mehek, N. Iqbal, T. Noor, H. Nasir, Y. Mehmood and S. Ahmed, Novel Co-MOF/graphene oxide electrocatalyst for methanol oxidation, *Electrochim. Acta*, 2017, **255**, 195–204.
- 77 P. Falcaro, *et al.*, A new method to position and functionalize metal-organic framework crystals, *Nat. Commun.*, 2011, **2**(1), 237.
- 78 O. M. Yaghi, M. J. Kalmutzki, and C. S. Diercks, *Introduction to Reticular Chemistry: Metal-Organic Frameworks and Covalent Organic Frameworks*, Wiley, 2019.
- 79 P. Falcaro, *et al.*, A new method to position and functionalize metal-organic framework crystals, *Nat. Commun.*, 2011, **2**(1), 1–8.
- 80 C. T. P. da Silva, *et al.*, Synthesis of Zn-BTC metal organic framework assisted by a home microwave oven and their unusual morphologies, *Mater. Lett.*, 2016, **182**, 231–234.
- 81 N. Qin, *et al.*, One-Step Construction of a Hollow Au@Bimetal-Organic Framework Core-Shell Catalytic Nanoreactor for Selective Alcohol Oxidation Reaction, *ACS Appl. Mater. Interfaces*, 2021, **13**(10), 12463–12471.
- 82 C.-L. Zhang, *et al.*, Core-shell structured porous carbon nanofibers integrated with ultra-small SnO<sub>2</sub> nanocrystals for fast and stable lithium storage, *Chem. Eng. J.*, 2021, **420**, 127705.
- 83 L. Zeng, *et al.*, Rational design of few-layer MoSe<sub>2</sub> confined within ZnSe-C hollow porous spheres for high-performance lithium-ion and sodium-ion batteries, *Nanoscale*, 2019, **11**(14), 6766–6775, DOI: 10.1039/C9NR00146H.
- 84 Z. Yan, *et al.*, Metal-organic frameworks-derived CoMOF-D@Si@C core-shell structure for high-performance lithium-ion battery anode, *Electrochim. Acta*, 2021, **390**, 138814.
- 85 M. Du, Q. Li, Y. Zhao, C.-S. Liu and H. Pang, A review of electrochemical energy storage behaviors based on pristine metal-organic frameworks and their composites, *Coord. Chem. Rev.*, 2020, **416**, 213341.
- 86 L. Shen, *Metal-Organic Frameworks-Based Electrolytes for Lithium Rechargeable Batteries*, University of California, Los Angeles, 2018.
- 87 Y. Zhang, *et al.*, Progress of electrochemical capacitor electrode materials: A review, *Int. J. Hydrogen Energy*, 2009, **34**(11), 4889–4899.
- 88 R. Boddula, M. I. Ahamed, and A. M. Asiri, *Applications of Metal-Organic Frameworks and Their Derived Materials*, Wiley, 2020.
- 89 X. Li, X. Yang, H. Xue, H. Pang and Q. Xu, Metal-organic frameworks as a platform for clean energy applications, *EnergyChem*, 2020, **2**(2), 100027.
- 90 X. Zou and G. Zhu, *Microporous Materials for Separation Membranes*, Wiley, 2019.
- 91 M. Bilal, S. Ashraf, M. Franco, D. S. Mulla and H. Iqbal, Harnessing the biocatalytic attributes and applied perspectives of nanoengineered laccases—A review, *Int. J. Biol. Macromol.*, 2020, **1**, 1.
- 92 M. Eddaoudi, H. Li and O. M. Yaghi, Highly Porous and Stable Metal-Organic Frameworks: Structure Design and Sorption Properties, *J. Am. Chem. Soc.*, 2000, **122**(7), 1391–1397.
- 93 Y. Xue, S. Zheng, H. Xue and H. Pang, Metal-organic framework composites and their electrochemical applications, *J. Mater. Chem. A*, 2019, **7**(13), 7301–7327, DOI: 10.1039/C8TA12178H.
- 94 X. Li, *et al.*, Metal-Organic Framework-Derived Carbons for Battery Applications, *Adv. Energy Mater.*, 2018, **8**(23), 1800716.
- 95 W. Shi, X. Xu, L. Zhang, W. Liu, and X. Cao, Metal-Organic Framework-Derived Structures for Next-Generation Rechargeable Batteries, *Functional Materials for Next-Generation Rechargeable Batteries*, 2021, pp. 179–200.
- 96 R. G. Compton and J. Wadhawan, *Electrochemistry: Nanoelectrochemistry*, Royal Society of Chemistry, 2013.
- 97 C. Zhang, *et al.*, Electrochemical performance of MIL-53 (Fe)@ RGO as an organic anode material for Li-ion batteries, *Electrochim. Acta*, 2017, **246**, 528–535.
- 98 P. George, K. Chaudhari and P. Chowdhury, Influence of cation doping (Li<sup>+</sup>, Na<sup>+</sup>, K<sup>+</sup>) on photocatalytic activity of MIL-53 (Fe), *J. Mater. Sci.*, 2018, **53**(16), 11694–11714.
- 99 A. Farisabadi, M. Moradi, S. Hajati, M. A. Kiani and J. P. Espinos, Controlled thermolysis of MIL-101 (Fe, Cr) for synthesis of Fe<sub>x</sub>O<sub>y</sub>/porous carbon as negative electrode and Cr<sub>2</sub>O<sub>3</sub>/porous carbon as positive electrode of supercapacitor, *Appl. Surf. Sci.*, 2019, **469**, 192–203.
- 100 F. Wang, H.-Y. Zhuo, X. Han, W.-M. Chen and D. Sun, Foam-like CoO@ N, S-codoped carbon composites derived from a well-designed N, S-rich Co-MOF for lithium-ion batteries, *J. Mater. Chem. A*, 2017, **5**(44), 22964–22969.
- 101 C. Li, *et al.*, The organic-moiety-dominated Li<sup>+</sup> intercalation/deintercalation mechanism of a cobalt-based metal-organic framework, *J. Mater. Chem. A*, 2016, **4**(41), 16245–16251.
- 102 W. Song, *et al.*, Rational construction of self-supported triangle-like MOF-derived hollow (Ni, Co) Se<sub>2</sub> arrays for electrocatalysis and supercapacitors, *Nanoscale*, 2019, **11**(13), 6401–6409.
- 103 M.-K. Song, S. Park, F. M. Alamgir, J. Cho and M. Liu, Nanostructured electrodes for lithium-ion and lithium-air batteries: the latest developments, challenges, and perspectives, *Mater. Sci. Eng., R*, 2011, **72**(11), 203–252.
- 104 P. Yang, *et al.*, Gel polymer electrolyte based on polyvinylidene fluoride-co-hexafluoropropylene and ionic liquid for lithium ion battery, *Electrochim. Acta*, 2014, **115**, 454–460.
- 105 S. Zeng, *et al.*, Graphene-supported highly crosslinked organosulfur nanoparticles as cathode materials for high-rate, long-life lithium-sulfur battery, *Carbon*, 2017, **122**, 106–113.
- 106 Y. Wang, *et al.*, Highly Branched VS<sub>4</sub> Nanodendrites with 1D Atomic-Chain Structure as a Promising Cathode Material for Long-Cycling Magnesium Batteries, *Adv. Mater.*, 2018, **30**(32), 1802563.
- 107 N. Wu, *et al.*, Cu<sub>2</sub>O/Cu@ C nanosheets derived from one novel Cu(II) metal-organic framework for high performance supercapacitors, *J. Alloys Compd.*, 2020, 157466.
- 108 L.-H. Zhang, Y. Zhu, B.-R. Lei, Y. Li, W. Zhu and Q. Li, Trichromatic dyes sensitized HKUST-1 (MOF-199) as





- scavenger towards reactive blue 13 via visible-light photodegradation, *Inorg. Chem. Commun.*, 2018, **94**, 27–33.
- 109 Q. Liu, *et al.*, Manganese-based layered coordination polymer: synthesis, structural characterization, magnetic property, and electrochemical performance in lithium-ion batteries, *Inorg. Chem.*, 2013, **52**(6), 2817–2822.
- 110 S. Maiti, A. Pramanik, T. Dhawa, M. Sreemany and S. Mahanty, Bi-metal organic framework derived nickel manganese oxide spinel for lithium-ion battery anode, *Mater. Sci. Eng., B*, 2018, **229**, 27–36.
- 111 Y. Li, *et al.*, MOF-derived Mn doped porous CoP nanosheets as efficient and stable bifunctional electrocatalysts for water splitting, *Dalton Trans.*, 2018, **47**(41), 14679–14685.
- 112 K. Zhang, *et al.*, Manganese based layered oxides with modulated electronic and thermodynamic properties for sodium ion batteries, *Nat. Commun.*, 2019, **10**(1), 1–12.
- 113 S. Shi, *et al.*, Full microwave synthesis of advanced Li-rich manganese based cathode material for lithium ion batteries, *J. Power Sources*, 2017, **337**, 82–91.
- 114 J. Lu, *et al.*, Photodynamic therapy for hypoxic solid tumors via Mn-MOF as a photosensitizer, *Chem. Commun.*, 2019, **55**(72), 10792–10795.
- 115 M. Zhang, X. Huang and Y. Chen, DFT insights into the adsorption of NH<sub>3</sub>-SCR related small gases in Mn-MOF-74, *Phys. Chem. Chem. Phys.*, 2016, **18**(41), 28854–28863.
- 116 Q. Zhang, B. Li and L. Chen, First-principles study of microporous magnets M-MOF-74 (M = Ni, Co, Fe, Mn): the role of metal centers, *Inorg. Chem.*, 2013, **52**(16), 9356–9362.
- 117 H. Jiang, Q. Wang, H. Wang, Y. Chen and M. Zhang, MOF-74 as an Efficient Catalyst for the Low-Temperature Selective Catalytic Reduction of NO<sub>x</sub> with NH<sub>3</sub>, *ACS Appl. Mater. Interfaces*, 2016, **8**(40), 26817–26826.
- 118 H. Li, *et al.*, Composite CD-MOF nanocrystals-containing microspheres for sustained drug delivery, *Nanoscale*, 2017, **9**(22), 7454–7463.
- 119 P. Xing, *et al.*, A Cd-MOF as a fluorescent probe for highly selective, sensitive and stable detection of antibiotics in water, *Analyst*, 2019, **144**(8), 2656–2661.
- 120 K. Wang, *et al.*, Porous Co–C core–shell nanocomposites derived from Co-MOF-74 with enhanced electromagnetic wave absorption performance, *ACS Appl. Mater. Interfaces*, 2018, **10**(13), 11333–11342.
- 121 Y.-C. Zhou, *et al.*, A new 3D 8-fold interpenetrating 66-dia topological Co-MOF: Syntheses, crystal structure, magnetic properties and electrocatalytic hydrogen evolution reaction, *J. Solid State Chem.*, 2019, **279**, 120929.
- 122 G. Huang, F. Zhang, L. Zhang, X. Du, J. Wang and L. Wang, Hierarchical NiFe<sub>2</sub>O<sub>4</sub>/Fe<sub>2</sub>O<sub>3</sub> nanotubes derived from metal organic frameworks for superior lithium ion battery anodes, *J. Mater. Chem. A*, 2014, **2**(21), 8048–8053.
- 123 C. Li, X. Hu and B. Hu, Cobalt(II) dicarboxylate-based metal-organic framework for long-cycling and high-rate potassium-ion battery anode, *Electrochim. Acta*, 2017, **253**, 439–444.
- 124 S. Mutahir, *et al.*, Pristine Co(BDC)TED<sub>0.5</sub> a pillared-layer biligand cobalt based metal organic framework as improved anode material for lithium-ion batteries, *Appl. Mater. Today*, 2020, **21**, 100813.
- 125 H. Song, L. Shen, J. Wang and C. Wang, Reversible lithiation–delithiation chemistry in cobalt based metal organic framework nanowire electrode engineering for advanced lithium-ion batteries, *J. Mater. Chem. A*, 2016, **4**(40), 15411–15419.
- 126 D. Ge, *et al.*, Nanostructured Co(II)-based MOFs as promising anodes for advanced lithium storage, *New J. Chem.*, 2016, **40**(11), 9238–9244.
- 127 J. Chen, X. Mu, M. Du and Y. Lou, Porous rod-shaped Co<sub>3</sub>O<sub>4</sub> derived from Co-MOF-74 as high-performance anode materials for lithium ion batteries, *Inorg. Chem. Commun.*, 2017, **84**, 241–245.
- 128 Y. Liao, *et al.*, Highly reversible lithium storage in cobalt 2,5-dioxido-1,4-benzenedicarboxylate metal-organic frameworks boosted by pseudocapacitance, *J. Colloid Interface Sci.*, 2017, **506**, 365–372.
- 129 S. Maiti, A. Pramanik, U. Manju and S. Mahanty, Cu<sub>3</sub>(1,3,5-benzenetricarboxylate)<sub>2</sub> metal-organic framework: A promising anode material for lithium-ion battery, *Microporous Mesoporous Mater.*, 2016, **226**, 353–359.
- 130 Z. Li, H. Liu, J. Huang and L. Zhang, MOF-derived α-MnSe/C composites as anode materials for Li-ion batteries, *Ceram. Int.*, 2019, **45**(17), 23765–23771.
- 131 L. Guo, J. Sun, X. Sun, J. Zhang, L. Hou and C. Yuan, Construction of 1D conductive Ni-MOF nanorods with fast Li<sup>+</sup> kinetic diffusion and stable high-rate capacities as an anode for lithium ion batteries, *Nanoscale Adv.*, 2019, **1**(12), 4688–4691.
- 132 S. Gao, R. Fan, B. Li, L. Qiang and Y. Yang, Porous carbon-coated ZnO nanoparticles derived from low carbon content formic acid-based Zn(II) metal-organic frameworks towards long cycle lithium-ion anode material, *Electrochim. Acta*, 2016, **215**, 171–178.
- 133 L. Hu, *et al.*, Lead-based Metal–Organic framework with stable lithium anodic performance, *Inorg. Chem.*, 2017, **56**(8), 4289–4295.
- 134 Y. Wang, *et al.*, Ultrasmall Fe<sub>3</sub>O<sub>4</sub> nanodots within N-doped carbon frameworks from MOFs uniformly anchored on carbon nanowebs for boosting Li-ion storage, *J. Mater. Chem. A*, 2018, **6**(8), 3659–3666.
- 135 C. Li, X. Lou, Q. Yang, Y. Zou and B. Hu, Remarkable improvement in the lithium storage property of Co<sub>2</sub>(OH)<sub>2</sub>BDC MOF by covalent stitching to graphene and the redox chemistry boosted by delocalized electron spins, *Chem. Eng. J.*, 2017, **326**, 1000–1008.
- 136 Z. Zhang, H. Yoshikawa and K. Awaga, Monitoring the solid-state electrochemistry of Cu(2,7-AQDC) (AQDC = anthraquinone dicarboxylate) in a lithium battery: Coexistence of metal and ligand redox activities in a metal–organic framework, *J. Am. Chem. Soc.*, 2014, **136**(46), 16112–16115.
- 137 W. Huang, *et al.*, A triphenylamine-based polymer with anthraquinone side chain as cathode material in lithium ion batteries, *Electrochim. Acta*, 2018, **283**, 1284–1290.



- 138 J. Xu, T. Lawson, H. Fan, D. Su and G. Wang, Updated Metal Compounds (MOFs, S, OH, N, C) Used as Cathode Materials for Lithium–Sulfur Batteries, *Adv. Energy Mater.*, 2018, **8**(10), 1702607.
- 139 T. Yamada, K. Shiraishi, H. Kitagawa and N. Kimizuka, Applicability of MIL-101(Fe) as a cathode of lithium ion batteries, *Chem. Commun.*, 2017, **53**(58), 8215–8218, DOI: 10.1039/C7CC01712J.
- 140 G. Férey, *et al.*, Mixed-valence Li/Fe-based metal–organic frameworks with both reversible redox and sorption properties, *Angew. Chem., Int. Ed.*, 2007, **46**(18), 3259–3263.
- 141 A. Fateeva, Synthesis, structure, characterization, and redox properties of the porous MIL-68 (Fe) solid, *Eur. J. Inorg. Chem.*, 2010, **24**, 3789–3794.
- 142 M. Nagarathinam, K. Saravanan, E. J. H. Phua, M. Reddy, B. Chowdari and J. J. Vittal, Redox-Active Metal-Centered Oxalato Phosphate Open Framework Cathode Materials for Lithium Ion Batteries, *Angew. Chem., Int. Ed.*, 2012, **51**(24), 5866–5870.
- 143 T. L. A. Nguyen, *et al.*, Reinvestigation of the MII (M = Ni, Co)/tetrathiafulvalenetetracarboxylate system using high-throughput methods: isolation of a molecular complex and its single-crystal-to-single-crystal transformation to a two-dimensional coordination polymer, *Inorg. Chem.*, 2010, **49**(22), 10710–10717.
- 144 K. Zhang, R. S. Varma, H. W. Jang, J.-W. Choi and M. Shokouhimehr, +Iron hexacyanocobaltate metal–organic framework: Highly reversible and stationary electrode material with rich borders for lithium-ion batteries, *J. Alloys Compd.*, 2019, **791**, 911–917.
- 145 W. Kaveevitchai and A. J. Jacobson, Exploration of vanadium benzenedicarboxylate as a cathode for rechargeable lithium batteries, *J. Power Sources*, 2015, **278**, 265–273.
- 146 J. Shin, *et al.*, MIL-101 (Fe) as a lithium-ion battery electrode material: a relaxation and intercalation mechanism during lithium insertion, *J. Mater. Chem. A*, 2015, **3**(8), 4738–4744.
- 147 T. Yamada, K. Shiraishi, H. Kitagawa and N. Kimizuka, Applicability of MIL-101 (Fe) as a cathode of lithium ion batteries, *Chem. Commun.*, 2017, **53**(58), 8215–8218.
- 148 B. Tian, *et al.*, Crystal engineering of naphthalenediimide-based metal–organic frameworks: structure-dependent lithium storage, *ACS Appl. Mater. Interfaces*, 2016, **8**(45), 31067–31075.
- 149 T. Yamada, K. Shiraishi and N. Kimizuka, Synthesis of a Redox-active Metal–Organic Framework MIL-116 (Fe) and Its Lithium Ion Battery Cathode Properties, *Chem. Lett.*, 2019, **48**(11), 1379–1382.
- 150 K. Zhang, R. S. Varma, H. W. Jang, J.-W. Choi and M. Shokouhimehr, + Iron hexacyanocobaltate metal–organic framework: Highly reversible and stationary electrode material with rich borders for lithium-ion batteries, *J. Alloys Compd.*, 2019, **791**, 911–917.
- 151 Z. Peng, X. Yi, Z. Liu, J. Shang and D. Wang, Triphenylamine-based metal–organic frameworks as cathode materials in lithium-ion batteries with coexistence of redox active sites, high working voltage, and high rate stability, *ACS Appl. Mater. Interfaces*, 2016, **8**(23), 14578–14585.
- 152 H. Nagatomi, N. Yanai, T. Yamada, K. Shiraishi and N. Kimizuka, Synthesis and Electric Properties of a Two-Dimensional Metal–Organic Framework Based on Phthalocyanine, *Chem.–Eur. J.*, 2018, **24**(8), 1806–1810.
- 153 S. Gu, Z. Bai, S. Majumder, B. Huang and G. Chen, Conductive metal–organic framework with redox metal center as cathode for high rate performance lithium ion battery, *J. Power Sources*, 2019, **429**, 22–29.
- 154 Q. Jiang, *et al.*, A Redox-Active 2D Metal–Organic Framework for Efficient Lithium Storage with Extraordinary High Capacity, *Angew. Chem.*, 2020, **132**(13), 5311–5315.
- 155 B. Tang, *et al.*, Mechanism of electrochemical lithiation of a metal–organic framework without redox-active nodes, *J. Chem. Phys.*, 2016, **144**(19), 194702.
- 156 A. S. Hameed, M. Nagarathinam, M. Schreyer, M. Reddy, B. Chowdari and J. J. Vittal, A layered oxalato phosphate framework as a cathode material for Li-ion batteries, *J. Mater. Chem. A*, 2013, **1**(18), 5721–5726.
- 157 Z.-Q. Du, Y.-P. Li, X.-X. Wang, J. Wang and Q.-G. Zhai, Enhanced electrochemical performance of Li–Co–BTC ternary metal–organic frameworks as cathode materials for lithium-ion batteries, *Dalton Trans.*, 2019, **48**(6), 2013–2018.
- 158 K. Saravanan, M. Nagarathinam, P. Balaya and J. J. Vittal, Lithium storage in a metal organic framework with diamondoid topology – a case study on metal formates, *J. Mater. Chem.*, 2010, **20**(38), 8329–8335, DOI: 10.1039/C0JM01671C.
- 159 W. Kaveevitchai, X. Wang, L. Liu and A. J. Jacobson, Two distinct redox intercalation reactions of hydroquinone with porous vanadium benzenedicarboxylate MIL-47, *Inorg. Chem.*, 2015, **54**(4), 1822–1828.
- 160 T. Yasuda and N. Ogihara, Reformation of organic dicarboxylate electrode materials for rechargeable batteries by molecular self-assembly, *Chem. Commun.*, 2014, **50**(78), 11565–11567.
- 161 V. Shrivastav, *et al.*, Metal–organic frameworks (MOFs) and their composites as electrodes for lithium battery applications: Novel means for alternative energy storage, *Coord. Chem. Rev.*, 2019, **393**, 48–78.
- 162 X. Zhang, A. Yuan, X. Mao, Q. Chen and Y. Huang, Engineered Mn/Co oxides nanocomposites by cobalt doping of Mn–BTC–New oxidase mimetic for colorimetric sensing of acid phosphatase, *Sens. Actuators, B*, 2019, **299**, 126928.
- 163 Y.-W. Li, *et al.*, Fe-MOF-Derived Efficient ORR/OER Bifunctional Electrocatalyst for Rechargeable Zinc–Air Batteries, *ACS Appl. Mater. Interfaces*, 2020, **12**(40), 44710–44719.
- 164 S.-L. Chou, J.-Z. Wang, H.-K. Liu and S.-X. Dou, Rapid synthesis of Li<sub>4</sub>Ti<sub>5</sub>O<sub>12</sub> microspheres as anode materials and its binder effect for lithium-ion battery, *J. Phys. Chem. C*, 2011, **115**(32), 16220–16227.
- 165 H. Liu, W. Li, D. Shen, D. Zhao and G. Wang, Graphitic carbon conformal coating of mesoporous TiO<sub>2</sub> hollow



- spheres for high-performance lithium ion battery anodes, *J. Am. Chem. Soc.*, 2015, **137**(40), 13161–13166.
- 166 H. Manjunatha, *et al.*, Electrochemical aspects of metal-organic frameworks, in *Metal-Organic Frameworks for Chemical Reactions*, Elsevier, 2021, pp. 65–109.
- 167 N. Angulakshmi, R. S. Kumar, M. A. Kulandainathan and A. M. Stephan, Composite polymer electrolytes encompassing metal organic frameworks: a new strategy for all-solid-state lithium batteries, *J. Phys. Chem. C*, 2014, **118**(42), 24240–24247.
- 168 W.-H. Li, W.-H. Deng, G.-E. Wang and G. Xu, Conductive MOFs, *EnergyChem*, 2020, **2**(2), 100029.
- 169 Y. Han, *et al.*, Metal-organic frameworks (MOFs) as sandwich coating cushion for silicon anode in lithium ion batteries, *ACS Appl. Mater. Interfaces*, 2015, **7**(48), 26608–26613.
- 170 C. Dong and L. Xu, Cobalt-and cadmium-based metal-organic frameworks as high-performance anodes for sodium ion batteries and lithium ion batteries, *ACS Appl. Mater. Interfaces*, 2017, **9**(8), 7160–7168.
- 171 D. Liu, Z. Jin and Y. Bi, Charge transmission channel construction between a MOF and rGO by means of Co-Mo-S modification, *Catal. Sci. Technol.*, 2017, **7**(19), 4478–4488.
- 172 C. Gerbaldi, *et al.*, Innovative high performing metal organic framework (MOF)-laden nanocomposite polymer electrolytes for all-solid-state lithium batteries, *J. Mater. Chem. A*, 2014, **2**(26), 9948–9954.
- 173 R. Dutta and A. Kumar, Structural and Dielectric Properties of Ionic Liquid Doped Metal Organic Framework based Polymer Electrolyte Nanocomposites–IOPscience, *J. Phys.: Conf. Ser.*, 2016, **765**, 012020.
- 174 C. Li, *et al.*, Hierarchical hollow Fe<sub>2</sub>O<sub>3</sub>@ MIL-101 (Fe)/C derived from metal-organic frameworks for superior sodium storage, *Sci. Rep.*, 2016, **6**(1), 1–8.
- 175 Z. He, *et al.*, MOF-derived hierarchical MnO-doped Fe<sub>3</sub>O<sub>4</sub>@ C composite nanospheres with enhanced lithium storage, *ACS Appl. Mater. Interfaces*, 2018, **10**(13), 10974–10985.
- 176 L. Wang, G. Zhang, Q. Liu and H. Duan, Recent progress in Zn-based anodes for advanced lithium ion batteries, *Mater. Chem. Front.*, 2018, **2**(8), 1414–1435.
- 177 G. Zheng, *et al.*, Controlling Surface Oxides in Si/C Nanocomposite Anodes for High-Performance Li-Ion Batteries, *Adv. Energy Mater.*, 2018, **8**(29), 1801718.
- 178 H. Jiang, C. Wang, H. Wang and M. Zhang, Synthesis of highly efficient MnO<sub>x</sub> catalyst for low-temperature NH<sub>3</sub>-SCR prepared from Mn-MOF-74 template, *Mater. Lett.*, 2016, **168**, 17–19.
- 179 S. Sun, *et al.*, Plasma modulated MOF-derived TiO<sub>2</sub>/C for enhanced lithium storage, *Chem. Eng. J.*, 2020, 128003.
- 180 T. Yao, *et al.*, Metal-Organic Framework Derived Ge/TiO<sub>2</sub>@C Nanotablets as High-Performance Anode for Lithium-Ion Batteries, *ChemistrySelect*, 2019, **4**(35), 10576–10580.
- 181 L. Li, L. Gu, Z. Lou, Z. Fan and G. Shen, ZnO quantum dot decorated Zn<sub>2</sub>SnO<sub>4</sub> nanowire heterojunction photodetectors with drastic performance enhancement and flexible ultraviolet image sensors, *ACS Nano*, 2017, **11**(4), 4067–4076.
- 182 B. Xue, K. Li, S. Gu, L. Zhang and J. Lu, Ni foam-supported ZnO nanowires and Co<sub>3</sub>O<sub>4</sub>/NiCo<sub>2</sub>O<sub>4</sub> double-shelled nanocages for efficient hydrogen peroxide detection, *Sens. Actuators, B*, 2018, **262**, 828–836.
- 183 T. Wang, *et al.*, A Co<sub>3</sub>O<sub>4</sub>-embedded porous ZnO rhombic dodecahedron prepared using zeolitic imidazolate frameworks as precursors for CO<sub>2</sub> photoreduction, *Nanoscale*, 2016, **8**(12), 6712–6720.
- 184 K. Huang, *et al.*, *In situ* anchoring of zeolite imidazole framework-derived Co, N-doped porous carbon on multiwalled carbon nanotubes toward efficient electrocatalytic oxygen reduction, *ACS Sustainable Chem. Eng.*, 2019, **8**(1), 478–485.
- 185 S. Salagare, P. Shivappa Adarakatti and Y. Venkataramanappa, Designing and construction of carboxyl functionalised MWCNTs/Co-MOFs-based electrochemical sensor for the sensitive detection of nitrite, *Int. J. Environ. Anal. Chem.*, 2020, 1–20.
- 186 J. Liu, *et al.*, ZnCo<sub>2</sub>O<sub>4</sub> nanoparticles derived from dual-metal-organic-frameworks embedded in Multiwalled Carbon Nanotubes: a favorable electrocatalyst for the water splitting, *Electrochim. Acta*, 2017, **257**, 233–242.
- 187 L. Jin, X. Zhao, X. Qian, S. Wang, X. Shen and M. Dong, Synthesis of porous In<sub>2</sub>O<sub>3</sub>/carbon composites derived from metal-organic frameworks for high performance Li-ion batteries, *Mater. Lett.*, 2017, **199**, 176–179.
- 188 Z. Zeng, H. Zhao, J. Wang, P. Lv, T. Zhang and Q. Xia, Nanostructured Fe<sub>3</sub>O<sub>4</sub>@ C as anode material for lithium-ion batteries, *J. Power Sources*, 2014, **248**, 15–21.
- 189 G. Chen, *et al.*, Solvothermal route based *in situ* carbonization to Fe<sub>3</sub>O<sub>4</sub>@ C as anode material for lithium ion battery, *Nano Energy*, 2014, **8**, 126–132.
- 190 P. Wang, *et al.*, A facile synthesis of Fe<sub>3</sub>O<sub>4</sub>/C composite with high cycle stability as anode material for lithium-ion batteries, *J. Power Sources*, 2013, **239**, 466–474.
- 191 Y. Liu, *et al.*, Metal organic frameworks derived porous lithium iron phosphate with continuous nitrogen-doped carbon networks for lithium ion batteries, *J. Power Sources*, 2016, **304**, 42–50.
- 192 Y. Tan, K. Zhu, D. Li, F. Bai, Y. Wei and P. Zhang, N-doped graphene/Fe-Fe<sub>3</sub>C nano-composite synthesized by a Fe-based metal organic framework and its anode performance in lithium ion batteries, *Chem. Eng. J.*, 2014, **258**, 93–100.
- 193 K. Zhou, L. Lai, Y. Zhen, Z. Hong, J. Guo and Z. Huang, Rational design of Co<sub>3</sub>O<sub>4</sub>/Co/carbon nanocages composites from metal organic frameworks as an advanced lithium-ion battery anode, *Chem. Eng. J.*, 2017, **316**, 137–145.
- 194 G. Huang, F. Zhang, X. Du, Y. Qin, D. Yin and L. Wang, Metal organic frameworks route to *in situ* insertion of multiwalled carbon nanotubes in Co<sub>3</sub>O<sub>4</sub> polyhedra as anode materials for lithium-ion batteries, *ACS Nano*, 2015, **9**(2), 1592–1599.



- 195 G. Zhang, *et al.*, High-performance and ultra-stable lithium-ion batteries based on MOF-derived ZnO@ ZnO quantum Dots/C core-shell nanorod arrays on a carbon cloth anode, *Adv. Mater.*, 2015, **27**(14), 2400–2405.
- 196 Q. Gan, K. Zhao, S. Liu and Z. He, MOF-derived carbon coating on self-supported ZnCo<sub>2</sub>O<sub>4</sub>-ZnO nanorod arrays as high-performance anode for lithium-ion batteries, *J. Mater. Sci.*, 2017, **52**(13), 7768–7780.
- 197 Z. Chen, *et al.*, Construction of hybrid hollow architectures by *in situ* rooting ultrafine ZnS nanorods within porous carbon polyhedra for enhanced lithium storage properties, *Chem. Eng. J.*, 2017, **326**, 680–690.
- 198 Q. Sun, *et al.*, Flakes-stacked Sn/SnO<sub>2</sub>/C composite as highly stable anode material for lithium-ion batteries, *J. Alloys Compd.*, 2020, 154677.
- 199 Y. Chen, Q. Huang, J. Wang, Q. Wang and J. Xue, Synthesis of monodispersed SnO<sub>2</sub>@ C composite hollow spheres for lithium ion battery anode applications, *J. Mater. Chem.*, 2011, **21**(43), 17448–17453.
- 200 M.-S. Wang, *et al.*, Scalable preparation of porous micron-SnO<sub>2</sub>/C composites as high performance anode material for lithium ion battery, *J. Power Sources*, 2016, **309**, 238–244.
- 201 F. Sun, *et al.*, A high performance lithium ion capacitor achieved by the integration of a Sn-C anode and a biomass-derived microporous activated carbon cathode, *Sci. Rep.*, 2017, **7**(1), 1–10.
- 202 Y. Guo, *et al.*, Sn nanoparticles encapsulated in 3D nanoporous carbon derived from a metal-organic framework for anode material in lithium-ion batteries, *ACS Appl. Mater. Interfaces*, 2017, **9**(20), 17172–17177.
- 203 X. Zhou, S. Chen, J. Yang, T. Bai, Y. Ren and H. Tian, Metal-organic frameworks derived okra-like SnO<sub>2</sub> encapsulated in nitrogen-doped graphene for lithium ion battery, *ACS Appl. Mater. Interfaces*, 2017, **9**(16), 14309–14318.
- 204 F. Marpaung, *et al.*, Metal-Organic Framework (MOF)-Derived Nanoporous Carbon Materials, *Chem.-Asian J.*, 2019, **14**(9), 1331–1343.
- 205 J. Gao, J. Ying, C. Jiang and C. Wan, High-density spherical Li<sub>4</sub>Ti<sub>5</sub>O<sub>12</sub>/C anode material with good rate capability for lithium ion batteries, *J. Power Sources*, 2007, **166**(1), 255–259.
- 206 Z. Lin, X. Hu, Y. Huai, L. Liu, Z. Deng and J. Suo, One-step synthesis of Li<sub>4</sub>Ti<sub>5</sub>O<sub>12</sub>/C anode material with high performance for lithium-ion batteries, *Solid State Ionics*, 2010, **181**(8–10), 412–415.
- 207 D. Mu, *et al.*, Nano-sized Li<sub>4</sub>Ti<sub>5</sub>O<sub>12</sub>/C anode material with ultrafast charge/discharge capability for lithium ion batteries, *J. Alloys Compd.*, 2016, **671**, 157–163.
- 208 Z. Wang, *et al.*, Porous anatase TiO<sub>2</sub> constructed from a metal-organic framework for advanced lithium-ion battery anodes, *J. Mater. Chem. A*, 2014, **2**(31), 12571–12575.
- 209 Z. Xiu, *et al.*, MOF-derived mesoporous anatase TiO<sub>2</sub> as anode material for lithium-ion batteries with high rate capability and long cycle stability, *J. Alloys Compd.*, 2016, **674**, 174–178.
- 210 Y. Liu, X. Zhao, F. Li and D. Xia, Facile synthesis of MnO/C anode materials for lithium-ion batteries, *Electrochim. Acta*, 2011, **56**(18), 6448–6452.
- 211 L. Yue, *et al.*, One-step solvothermal process of In<sub>2</sub>O<sub>3</sub>/C nanosheet composite with double phases as high-performance lithium-ion battery anode, *Electrochim. Acta*, 2015, **160**, 123–130.
- 212 L. Yu, *et al.*, Metal-organic framework-derived NiSb alloy embedded in carbon hollow spheres as superior lithium-ion battery anodes, *ACS Appl. Mater. Interfaces*, 2017, **9**(3), 2516–2525.
- 213 J. Li, *et al.*, Cu-MOF-Derived Cu/Cu<sub>2</sub>O Nanoparticles and CuN<sub>x</sub>C<sub>y</sub> Species to Boost Oxygen Reduction Activity of Ketjenblack Carbon in Al-Air Battery, *ACS Sustainable Chem. Eng.*, 2018, **6**(1), 413–421.
- 214 D. Ji, *et al.*, Facile fabrication of MOF-derived octahedral CuO wrapped 3D graphene network as binder-free anode for high performance lithium-ion batteries, *Chem. Eng. J.*, 2017, **313**, 1623–1632.
- 215 Q. Liu, *et al.*, Double Coating of Micron-Sized Silicon by TiN@ NC for High-Performance Anode in Lithium-Ion Batteries, *Energy Technol.*, 2019, **7**(9), 1900487.
- 216 C. Liu, R. Tian, D. Sun, H. Liu and H. Duan, MOF-derived 3D hollow porous carbon/graphene composites for advanced lithium-ion battery anodes, *J. Solid State Chem.*, 2020, **290**, 121568.
- 217 R. Guo and W. Wu, Recent Advances in Graphene Lithium-Ion Batteries, *Gen. Chem.*, 2016, **2**(2), 66–83.
- 218 L. Wang, X. Li, Z. Tang and X. Zhang, Research on Li<sub>3</sub>V<sub>2</sub>(PO<sub>4</sub>)<sub>3</sub>/Li<sub>4</sub>Ti<sub>5</sub>O<sub>12</sub>/C composite cathode material for lithium ion batteries, *Electrochem. Commun.*, 2012, **22**, 73–76.
- 219 W. Kim, M. Choi and K. Yong, Generation of oxygen vacancies in ZnO nanorods/films and their effects on gas sensing properties, *Sens. Actuators, B*, 2015, **209**, 989–996.
- 220 K. Shiva, K. Jayaramulu, H. Rajendra, T. Kumar Maji and A. J. Bhattacharyya, *In situ* Stabilization of Tin Nanoparticles in Porous Carbon Matrix derived from Metal Organic Framework: High Capacity and High Rate Capability Anodes for Lithium-ion Batteries, *Z. Anorg. Allg. Chem.*, 2014, **640**(6), 1115–1118.
- 221 Q. Guo, Z. Zheng, H. Gao, J. Ma and X. Qin, SnO<sub>2</sub>/graphene composite as highly reversible anode materials for lithium ion batteries, *J. Power Sources*, 2013, **240**, 149–154.
- 222 F. Zou, *et al.*, Metal organic frameworks derived hierarchical hollow NiO/Ni/graphene composites for lithium and sodium storage, *ACS Nano*, 2016, **10**(1), 377–386.
- 223 C. Zhang, Q. Zhang, K. Zhang, Z. Xiao, Y. Yang and L. Wang, Facile synthesis of a two-dimensional layered Ni-MOF electrode material for high performance supercapacitors, *RSC Adv.*, 2018, **8**(32), 17747–17753.
- 224 R. Yang, *et al.*, Efficient electromagnetic wave absorption by SiC/Ni/NiO/C nanocomposites, *J. Alloys Compd.*, 2020, **816**, 152519.

